Stony Brook University

An in vitro study of the anti-biofilm properties of proanthocyanidin and chitosan in *Pseudomonas syringae* pv. *papulans*

A Thesis Presented

by

Kai Song

to

The Graduate School

in Partial Fulfillment of the

Requirements

for the Degree of

Master of Science

in

Materials Science and Engineering

Stony Brook University

May 2013

Stony Brook University

The Graduate School

Kai Song

We, the thesis committee for the above candidate for the

Master of Science degree, hereby recommend

acceptance of this thesis.

Yizhi Meng – Thesis Advisor,
Assistant Professor, Materials Science and Engineering

Dilip Gersappe – Committee Member,
Professor, Graduate Program Director, Materials Science and Engineering

Elizabeth Boon-Committee Member,
Assistant Professor, Chemistry

This thesis is accepted by the Graduate School

Charles Taber
Interim Dean of the Graduate School

Abstract of the Thesis

An in vitro study of the anti-biofilm properties of proanthocyanidin and chitosan in *Pseudomonas syringae* pv. *papulans*

by

Kai Song

Master of Science

in

Materials Science and Engineering

Stony Brook University

2013

Biofilm-forming bacteria are a form of planktonic microorganisms that can become resistant against conventional antibiotics. Because they are difficult to eradicate, biofilm-forming bacteria are extremely problematic for the medical industry areas. Thus, materials that can distort biofilm structure would be helpful for eliminating chronic infection and decreasing bacterial resistance. The primary objective of this study is to evaluate the anti-biofilm effect of two bio-derived substances, proanthocyanidin and chitosan. Proanthocyanidins are secondary plant metabolites that are reported to have antibiotic and antioxidant functions. Chitosan (poly [β-(1, 4)-amino-2-deoxy-β-D-glucose]) is a deacetylated derivative of chitin, which is abundant in the exoskeleton of crustaceans and insects. It is reported to be a suitable substitute for conventional fungicides and can enhance the proanthocyanidin content in plants when used as an agrochemical. Chitosan-tripolyphosphate (TPP) nanoparticles, which have good neutral water solubility and are nanoscale in size, can be used as carriers for gene and drug therapy and are thus favorable to be

tested as a treatment method against bacterial biofilms. In this study, the anti-biofilm and antibacterial properties of proanthocyanidin, chitosan-TPP nanoparticles and proanthocyanidins-loaded chitosan-TPP nanoparticles were tested using the model plant bacterium, *Pseudomonas syringae* pv. *papulans* (Psp), a pathogen isolated from infected apples. At a lower concentration (1 mg/mL and 2.5 mg/mL), both chitosan nanoparticles and proanthocyanidins can postpone the formation of biofilms and eventually disrupted part of the biofilm. While higher concentration (above 5 mg/mL) of chitosan nanoparticles or proanthocyanidins can eliminate most of the biofilm in this study. PAC-loaded chitosan nanoparticles also can also distort biofilms. Both proanthocyanidins and chitosan-TPP nanoparticle showed a mild antibacterial property. PAC-loaded chitosan-TPP nanoparticle exhibited a stronger and durable antibacterial property.

Table of Contents

Lists of Tables

Lists of Figures

List of Abbreviations

PAC: proanthocyanidins

CSNPs: chitosan nanoparticles

ZoI: zone of inhibition

Acknowledgments

I am grateful to Prof. Yizhi Meng, my graduate advisor, who provided precious advices to me. She continually conveyed interest and rigor in regard to research and scholarship, and patience and enthusiasm in regard to teaching. She can always find a balance between strict requirement and cheerful encouragement. This thesis would not have been finished without your guidance.

Besides my advisor, I would thank my committee members, Prof. Dilip Gersappeand Prof. Elizabeth Boon for their insightful guidance and comments.

Besides, I want to thank all the laboratory members from Dr. Meng's group who helped and worked with me. They are Kathryn Dorst, Giulia Suarato, Cheng Zhang, Gaojun Liu, Xin He Amanda Chin, Junyi Wu and Derek Rammelkamp. We spent a delight time together. Also, I wish to thank two research volunteers in my project, Xiuming Chen and Niveditha Obla, who offered a lot of help and suggestions to me.

I would also express my thanks to Shelagh Zegers from department of Marine science and Dmytro Nykypanchuk from Center for Functional Nanomaterials of Brookhaven National Laboratory for their assistance to my project.

Last but not the least, I would like to express my sincere gratitude to my parents, Jianghu Song and Yunxia Li, who bring me up and fully support my entire academic life. They are the first two advisors in my life.

1 Review of the Literature

1.1 Antibiotic resistance

Antibiotics refer to a class of compounds that can kill or restrict the growth of bacteria or other pathogenic microorganisms. Interestingly, most of these antibiotics are also derivatives of natural substances. Penicillin, the first antibiotic, was discovered by Sir Alexander Fleming in 1928. It is derived from Penicillium fungi and showed significant antibacterial function towards many serious diseases at that time. Different forms of natural, semisynthetic, and synthetic antibiotics have been discovered since then. There are more than 50 penicillins, 70 cephalosponns, 12 tetracyclines, 8 aminoglycosides, 1 monobactam, 3 carbapenems, 9 macrolides, 2 new streptogramins, and 3 dihydrofolate reductase inhibitors [3].

Generally, antibiotics act via the following mechanisms: inhibition of protein synthesis or damage to cell wall, cytoplasmic membrane, protein synthesis, inhibition of synthesis or metabolism of nucleic acid, and modification of energy metabolism [4].

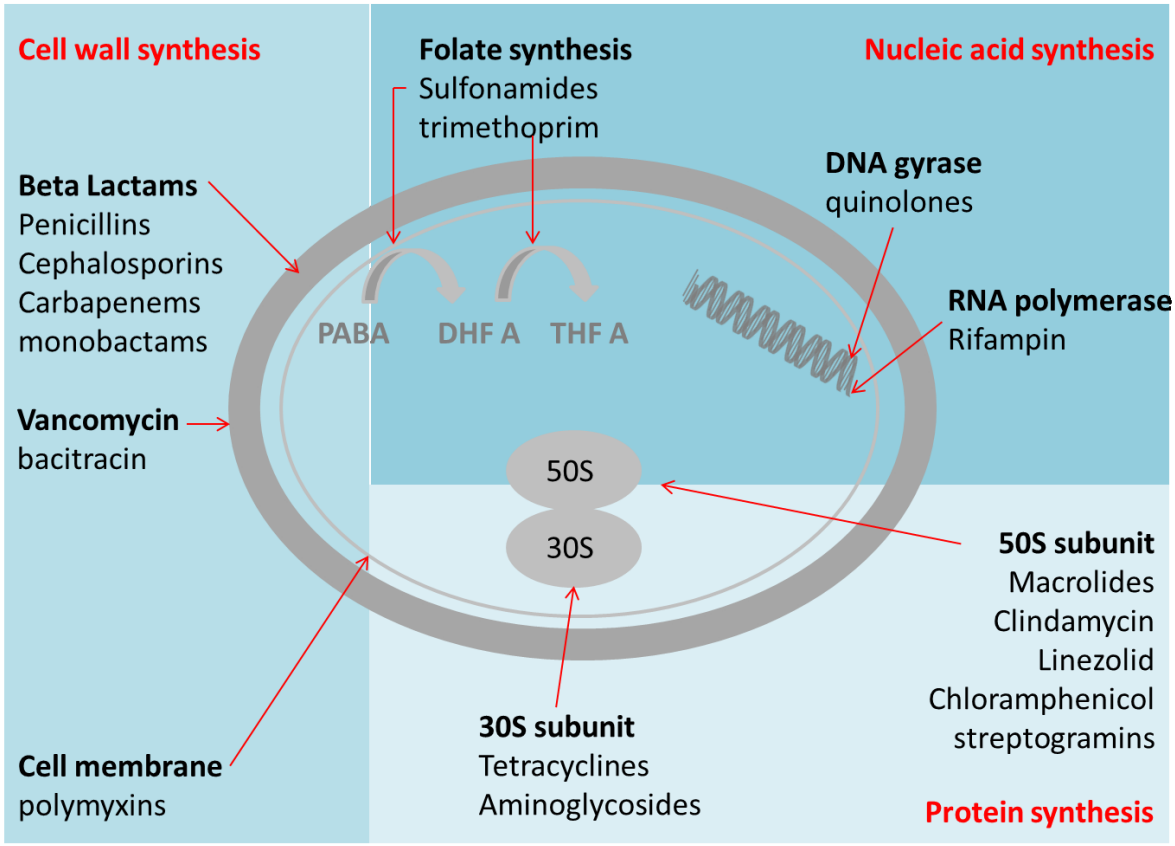

Fig.1 Sites of action of various antibiotics (modified from [4])

However, a new problem is surfacing due to the wide application of antibiotics— that of bacterial resistance. In 1941 almost all strains of *Staphylococcus aureus* were susceptible to penicillin G in the world. But in 1943 *Staphylococcus aureus* was found to be able to undergo enzymolysis through penicillinase.[1].Today, more than 95% of *Staphylococcus aureus* strains are resistant to penicillin, ampicillin, and the antipseudomonas penicillins[2]. Another example is *Pneumococci bacteria* which are a major cause of community-acquired pneumonia, otitis media, sinusiris, and meningitis both in children and adults. In 1941, the dose of penicillin for these bacteria was 10,000 units per day; while 50 years later, the dose increased remarkably to 24

million units per day [5]. Research has shown that bacteria gain antibiotic resistance via gene mutation through the exchange of DNA, transduction, or conjugation by plasmids [4].

1.2 Biofilm formation and hazard

1.2.1 Biofilm formation

Bacterial biofilms are communities of microorganism that attach on a surface and are protected by a matrix of self-produced extracellular polymeric substance (EPS), which is different from planktonic bacterial cells. Biofilms basically consist of polysaccharide, protein, and nucleic acid [6-9]. Biofilms were firstly discovered early as the mechanism for bacteria to interact with outer environment, but it was not until the late 20th century that its significance was realized [5]. Biofilm-related hazards cost billions of loss in economy from marine industry to medical systems.

Generally, the formation of biofilms occurs in five stages:

1. The planktonic bacteria cells attach unstably to the living or non-living surface. Whether the bacteria would come to a more stable statue depends on the environmental condition. The suitable condition would send a signal to the attached bacteria, which would initiate the alteration of gene expression. At this stage, the bacteria are more vulnerable to the antibiotic. Once the bacteria enter stage B, the process would become irreversible.

2. The cells begin to proliferate and produce the extracellular polymeric substance (EPS). This complex, highly polar matrix would protect the residential bacterial cells from antibiotics

and host immune responses [10]. It is essential to prevent bacteria from forming biofilm at earlier stage. Once biofilm is formed, it is a virtual impossibility to remove it all.

3. EPS continues to grow during the third stage, making the biofilm thicker and stickier.

4. The biofilm becomes mature and grows in three-dimension. In this tridimensional structure, some micro tunnels appear, which could facilitate the transport of water, nutrients and waste. This also causes the more cavities to culture more planktonic bacteria. Furthermore, this semi-isolated structure would promote more mutation and gene transference, which increase the resistant rate [11-14].

5. Once the biofilms become fully mature, the structure begins to fracture and release planktonic bacterial cells to the environment and a new circle begins [15,16]. The theory of persistor cells proposed that a small group of bacteria may survive in the application of antibiotics and subsequently reconstruct the biofilm. The surviving bacteria have a higher chance to produce descendants with antibiotic resistance. The biofilms and persistor bacteria benefit each other, leading to a more difficult treatment each time [7-9].

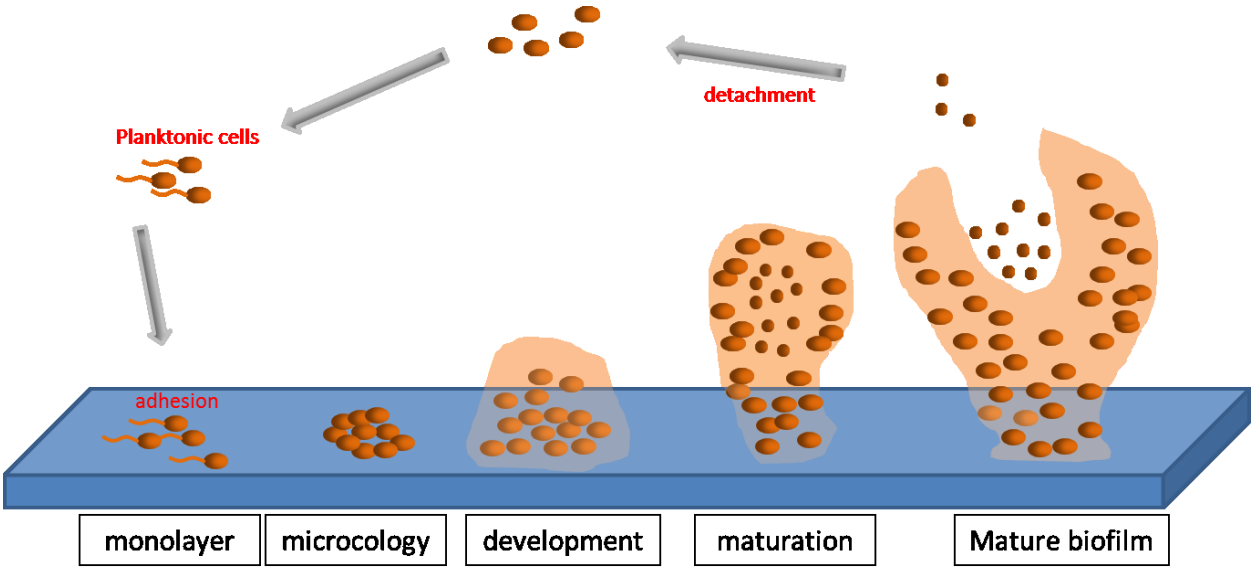

Fig.2 Cycle of biofilm formation (modified from [5])

1.2.2 Biofouling

Biofilm hazard refers to biofouling which involves the growth of these biofilms on the surfaces of commercial equipment causing costly energy losses, physical damage and chemical contamination in variety of industries [11-13]. In the paper milling industry, for example, the production line provides good condition for biofilm formation—many biodegradable materials (wood, starch), suitable temperature (25-50°C), free access to water and air. Such biofilms would cause clogging of filters, sheet breaks or holes in the paper [20]. In the shipping industry, biofilm formation on the surface of ships would increase sailing resistance and decrease ship maneuverability which ultimately increases energy consumption and equipment depreciation rate [22]. In long term, waste products and metabolites released from biofilm would lead to bio-corrosion and coordinate with natural corrosion, which result in larger damage.

1.2.3 Biofilm hazard in health

Recently, biofilms have been found in 80% bacterial infections and a wide range of chronic diseases [24]. Dental diseases such as cavities are mainly caused by biofilms and corrosive waste of parasitic bacteria (mainly *Streptococcus mutans* and *Streptococcus sanguinis*). The oral environment provides ideal conditions (air, water, nutrition, and habitat) and biofilms provide protection against tooth brushing and antibiotics. The high concentration of microorganisms in teeth and gingival tissues makes this disease a long-term affliction [25]. Many chronic lung diseases are also caused by biofilms mediated infections. The bacterium *Pseudomonas aeruginosa* is a major lung pathogen and can cause infection in the lung permanently even under powerful antibiotics [26-28]. It is strongly suggested this bacterium forms polymeric biofilms in the cystic fibrotic lung [26, 29]. Some more serious and costly cases occur when the indwelling medical device (IMD) gets infected by bacteria. Biofilms formed inside the body cannot be killed thoroughly by regular antibiotics, resulting in fiercely physiological reaction in vivo. Additional surgeries are needed to take out the devices to clean the infected area or replace with a new one [30].

1.2.4 Commercial anti-biofilm methods

The basic method to prevent biofilm-forming bacteria in commercial equipment is to apply chemical substances that are resistant to bacteria attachment. Coating the submerged surfaces of a ship with heavy metal or organotins was once successful but is banned now because of their high toxicity toward marine biosphere [53]. These chemicals accumulate in fish and shellfish, resulting in higher accumulations in their predators and humans [31]. In medical system, different antibiotics and chemicals, such as cefazolin, rifampin/minocycline and silver/chlorohexidine, are investigated as antibiofilm coating substances; but many of them may have the risk to develop resistance of bacterial resistance [5].

1.3 Proanthocyanidins

Proanthocyanidins belong to a class of polyphenols, flavanols. They are widely distributed in the plant kingdom such as barks, leaves, fruits and seeds. It is reported that they possess a higher concentration in grape seeds, grape skins, red wine of *Vitis vinifera* (a common species of grape), apples, maritime pine bark, cinnamon, and cocoa beans.[36,37]

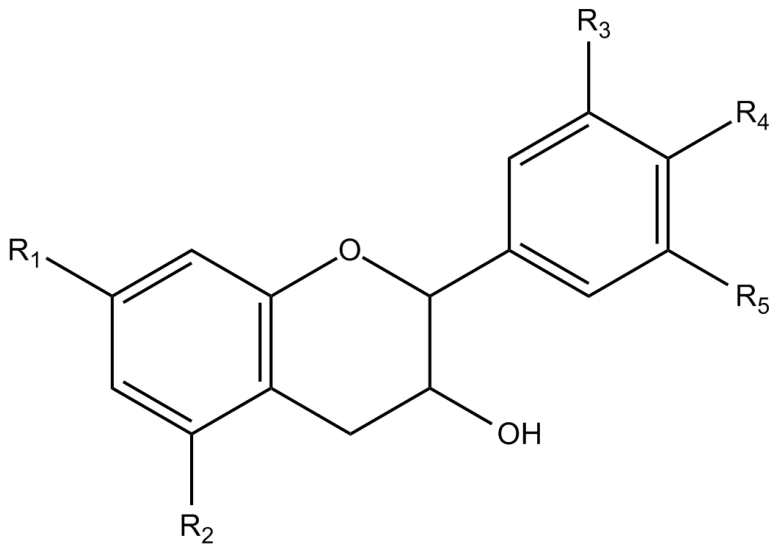

Catechin (R_1=R_2=R_3=R_4=OH;R_5=H)
Gallocatechin (R_1=R_2=R_3=R_4=R_5=OH)

Fig.3 Basic unit structure of flavanols (modified from [34])

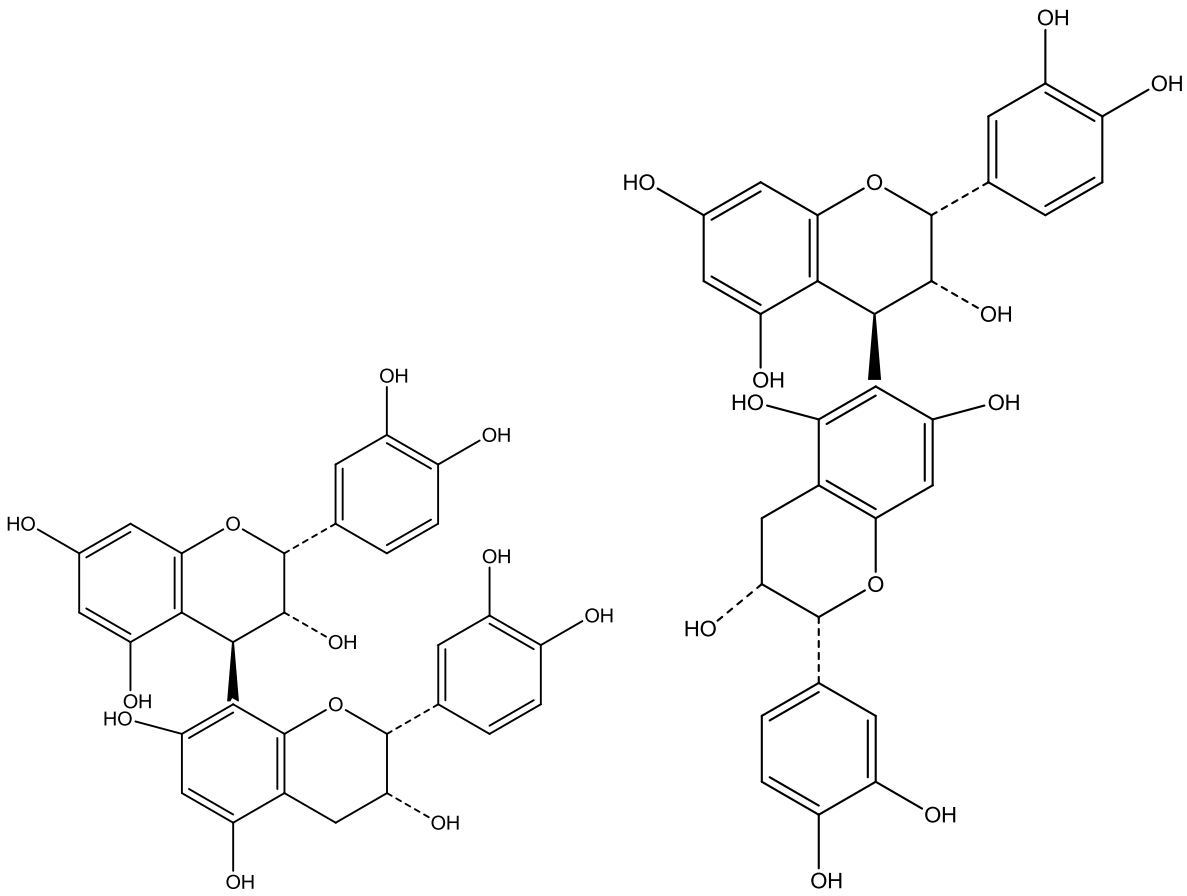

Fig.4 General subunit structures of proanthocyanidins (modified from [34])

1.3.1 Health benefits of proanthocyanidin

Proanthocyanidins have been revealed to have several health benefits. Most studies dealing with quantitative chemical analyses point out that proanthocyanidins could be the main contributors to perceived astringency in wine due to their ability to precipitate salivary proteins.[38] Proanthocyanidins are also reported as a significant antioxidant and their anti-oxidation capacity is about 50 times that of Vitamin C. Tomato Lycopene and Astaxanthin show higher anti-oxidation capacity than proanthocyanidins but their fat-soluble makes them less potential in aqueous system. The oxidation of low-density lipoprotein (LDL) in artery is considered the mainly cause of the formation of the atherosclerotic plaque. Shanmuganayagam et

al. found that with the application of proanthocyanidins (Degree of Polymerization between 3-15), the lagtime of LDL can be increased between 300% and 400%.[39] Grape seed extract (GSE), of which proanthocyanidins is a major component, has been reported to be able to reduce blood pressure. One recent study claims that in a series of trials conducted at the University of California at Davis medical school both the systolic and diastolic blood pressures were lowered after treatment with commercial GSE at a dose of 150mg or 300 mg per day as compared with placebo [40].

1.3.1.1 Antibacterial and anti-biofilm research on Proanthocyanidins

Proanthocyanidins belong to the class of polyphenols which are shown to have an important role in promoting plant growth and reproduction, as well as protecting the plants from diseases and predators [41]. Antibacterial and antibiofilm ability of polyphenols especially proanthocyanidins have been investigated by different research groups [42-45]. Robert Mayer et al., first optimized the extraction of different fractions through a microwave-assisted process, then analyzed different fractions through high-performance liquid chromatography-mass spectrometry (HPLC). These fractions (proanthocyanidins, monomeric flavonoid, and their glycosides) were tested against ten different Gram-positive and Gram-negative bacteria strains. They found that proanthocyanidins and gallate esters were the effective substances among these fractions [45]. Daglia et al. found that proanthocyanidins in de-alcoholized red wine, also showed antibacterial activities as well as significant antibiofilm function towards *Streptococcus mutans* [46].

1.4 Chitosan

Chitosan (poly [β-(1,4)-amino-2-deoxy-β-D-glucose]) is a natural biopolymer that is nontoxic, biocompatible, and biodegradable [47]. It is a deacetylaed derivative of chitin, which is distributed widely in natural organisms such as exoskeleton of crabs and insects, cell walls of fungi, and beaks of birds.

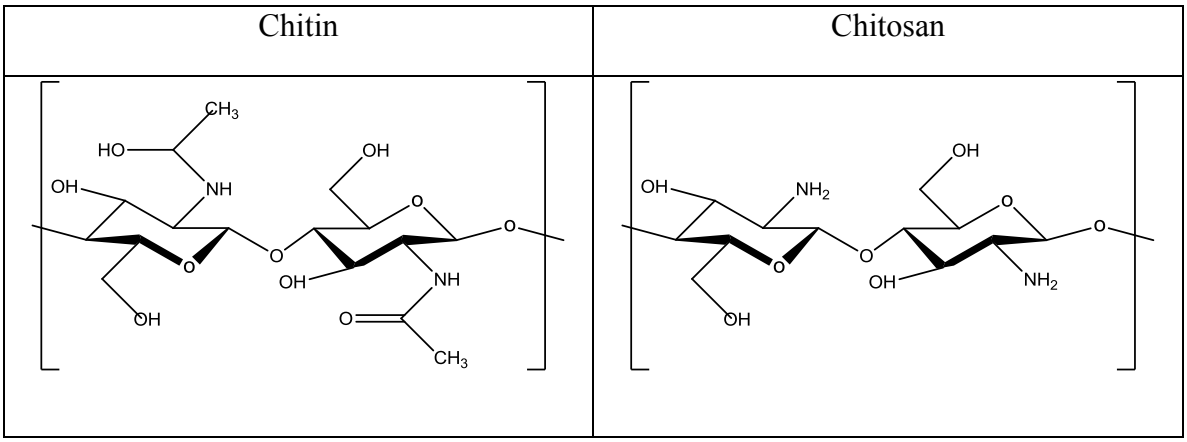

Fig.5 The chemical structures of chitin and chitosan

1.4.1 Bulk chitosan vs. chitosan nanoparticles

The antibacterial activity of chitosan and its derivatives are widely reported. Chitosan, as a biopolymer and a deacetylation derivative, has a wide range of molecular weight (Mw) and degree of deacetylation (DD). Thus the antibacterial ability of chitosan may vary from its Mw and DD. Aharya et al. reported that chitosan with a higher DD had a higher adherence to bacterial cells, and thus also a higher antibacterial function. Liu et al. found that Mw of Chitosan must be under about 5000 Da if chitosan is expected to penetrate cell membrane [51]. The pH of the medium and concentration of chitosan are also showed having effects on the antibacterial

action of chitosan. Liu further found that under neutral or basic environment, chitosan barely showed any antibacterial activity, due to its poor solubility [51].

There are several suggestions about the mechanism of the antibacterial activity of chitosan. Chung suggested that because of the negative charge of cell surfaces, the positively charged chitosan can interfere with the cell by adhering to the surface. It is also suggested that the more negative the cell surface, the stronger the interaction would be between it and cells [48]. Once chitosan becomes attached to the cell wall, cell permeability may change, which may lead to the decline and death of cells [49]. Hadwinger et al. suggested that chitosan can penetrate cell surfaces and combine with DNA molecules to further impede RNA transcription [50].

1.4.2 Antibiofilm properties of chitosan

Anil Kisben et al. prepared chitosan nanoparticle (CSNPs) with the average diameter of 70 nm, DD of 84%, and zeta potential of 49mv. CSNPs showed strong antibacterial activity towards the test bacteria (*E. faecalis*) by killing the bacteria completely within 8 hours. The CSNPs also showed good antibiofilm action. After the canal dentin was treated with CSNPs, it showed about 80% reduction in bacterial adherence. In further experiments, CSNPs was also incorporated with zinc oxide nanoparticles, which exhibited better antibacterial and antibiofilm activities [52]. Jena et al. found that chitosan-stabilized Ag nanoparticles showed antibacterial actions toward wide spectrum of human bacteria without killing human cell and can prevent biofilm formation [53].

Despite its antibacterial properties, chitosan may still be less effective compared with traditional synthetic antiseptics. Decker et al. compared four compounds (chlorhexidine, Olaflur, Octenisept and Chitosan) and tested the bacterial viability of planktonic or attached *Streptococci* with or without sample compound treatment. Results of antibacterial and antibiofilm tests

showed that chitosan had lower inhibitory activity than the three synthetic commercial compounds [54].

2 Objective

These reports gave rise to the idea that a combination of chitosan and proanthocyanidins, both of which are revealed to have antibacterial and antibiofilm functions, may have synergistic effects against biofilm-forming microorganisms. The objectives of this thesis are:

(1) To synthesis and characterize chitosan-tripolyphosphate nanoparticles and proanthocyanidins-loaded chitosan-tripolyphosphate nanoparticles.

(2) To evaluate the anti-biofilm properties of proanthocyanidins, bulk chitosan, chitosan-tripolyphosphate nanoparticles and proanthocyanidins-loaded chitosan-tripolyphosphate nanoparticle in vitro.

(3) To evaluate the synergistic antibacterial properties of proanthocyanidins and chitosan-tripolyphosphate nanoparticles

3 Methods

3.1 Synthesis of chitosan-tripolyphosphate (TPP) nanoparticle

3.1.1 Synthesis of chitosan-TPP nanoparticle

In this experiment, Chitosan-tripolyphosphate nanoparticles were synthesized using the ionic gelation method according to Lifeng Qi's work [59] with modification (Fig.6). Acetic acid (J.T.Baker) was firstly diluted in distilled water to make a 1% v/v solution. Sodium tripolyphosphate (technical grade, 85%, Sigma-Aldrich) was prepared into 0.25% w/v solution. Then 0.5g chitosan powder (lower molecular, deacetylation degree 75%-85%, Sigma-Aldrich) was added to 100 mL acetic acid solution, followed by stirring for 2 hours. The pH value of chitosan solution was adjusted between 4.6 and 4.8 by 10 M NaOH. Afterwards, 33.3 mL TPP solution was added dropwise. These previous processes were all completed at room temperature. The synthesized nanoparticle suspension was centrifuged at 2700 rpm for 30 min and rinsed with DI water. The solution was kept in freezer at -80°C for 48 hours and then freeze dried for 48 hours. 5% trehalose (Sigma) was added to prevent the nanoparticles from aggregating during the freeze-drying process. The freeze dried sample was collected, grinded with a mortar and pestle, and stored in a 20 ml glass vial.

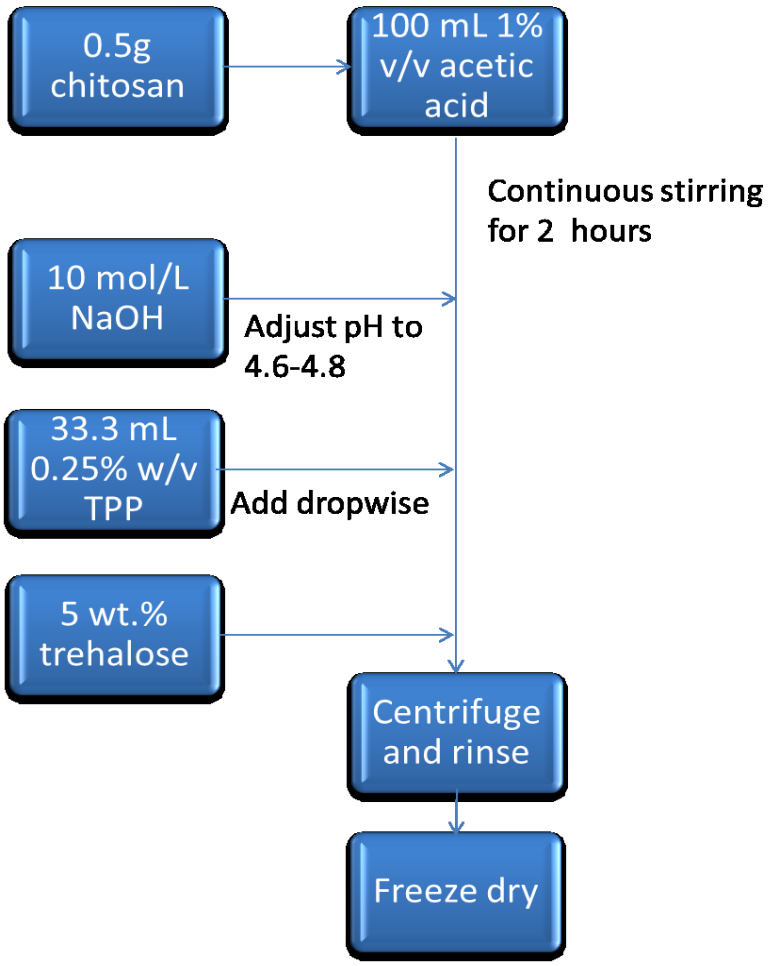

Fig.6 Procedures to prepare chitosan-TPP nanoparticles

3.1.2 Synthesis of proanthocyanidins-loaded chitosan-TPP nanoparticles

Preparation of proanthocyanidins-loaded chitosan-TPP nanoparticles is similar to the preparation of chitosan-TPP nanoparticles as mentioned in section 3.1.1. One hundred milliliters of 1% acetic acid with 0.5 g chitosan was under stirring for 2 hours. Ten milliliters of proanthocyanidins solution in 100% ethanol were then added. The pH value of chitosan-proanthocyanidin mixture was then adjusted between 4.6 and 4.8 by 10 M NaOH. Afterwards, 33.3 mL TPP solution was added dropwise. These procedures were under stirring at room temperature. Then the nanoparticles were precipitated through centrifuge for 30 minutes and

neutralized by rinsing with DI water three times. The PAC-loaded chitosan-TPP nanoparticles solution in DI water was stored in dark under nitrogen environment.

3.2 Preparation of proanthocyanidins stock solution

MegaNatural® - BP Grape extract tablets were purchased from Endurance Products Company (Madera, CA). The tablets were firstly ground by a mortar and pestle set. Then the grape seed powder was dissolved into either autoclaved DI water or Terrific Broth in 50 mL Falcon® tubes (BLUE MAX™ Jr. 15 mL Polystyrene Conical Tube, 17×120mm style, sterile). The solution was then vortexed for 5 min and sonicated for 8 min. After that, the solution was passed through 0.2 μm syringe filter. The solution was kept under the nitrogen and in the dark to avoid oxidation.

3.3 Preparation of gauze bandage with chitosan nanoparticles and PAC-loaded chitosan nanoparticles

The gauze bandage was cut into 2.5 cm x 2.5 cm in width squares followed by sterilization through autoclave. The bandages were firstly soaked with autoclaved DI water for 30 minutes, and then soaked with sterile filtered nanoparticle suspension overnight. The bandages were then transferred petri dishes and left to airdry for three hours. After that, the bandages were placed onto the agar plates fleshly streaked with *Pseudomonas syringae* pv. *papulans*. The plates imaged using a photo scanner on a daily basis and the zone of inhibition was measured.

3.4 Material characterization

3.4.1 Particle size and zeta potential of Chitosan-TPP nanoparticles

The particle size of chitosan-TPP was measured by dynamic light scattering (DLS) as follows. The 1mg/mL chitosan-TPP nanoparticle solution and as-prepared PAC-loaded chitosan-TPP nanoparticle solution were prepared and sonicated for 10 min. The nanoparticle solutions were then immediately analyzed by a Malvern Zetasizer Nano at the Center for Functional Nanomaterial at Brookhaven National Lab (Upton, NY). The measurements were performed in triplication.

The zeta potential was also measured by the Malvern Zetasizer Nano. The 1mg/mL chitosan-TPP nanoparticle solution and as-prepared PAC-loaded chitosan-TPP nanoparticle solution were prepared and sonicated for 10 min. Then 200 μL of nanoparticle solutions were injected into a zeta dip cell and measured in triplication.

3.4.2 Transmission electron microscope imaging of PAC-loaded chitosan nanoparticles

The TEM images were measured by JEOL JEM-1400 LaB6 120KeV Transmission Electron Microscope at the Center for Functional Nanomaterial at Brookhaven National Lab (Upton, NY). The sample used was as-prepared as-prepared PAC-loaded chitosan-TPP nanoparticle solution

3.4.3 Determination of chitosan concentration in lyophilized chitosan-TPP nanoparticle powders

Because chitosan-TPP nanoparticles were freeze-dried with trehalose, the precise precise chitosan content needed was to be measured. The method was modified from Emilia Curotto's

protocol [57]. A 2% solution of Ninhydrin (2, 2-Dihydroxyindane-1, 3-Dione) was used to determine the concentration of chitosan in chitosan-TPP powder. A 0.1 mg /mL chitosan solution in 1 % acetic acid was firstly prepared. A series of chitosan solutions were then mixed with ninhydrin solution in five tubes as shown in table 1. The tubes were kept in boiling water for 15 minutes and cooled down to room temperature. A 2 mL aliquot of 99% ethanol was added to each tube, followed by gentle shaking to mix homogeneously. A 200 µL aliquot was extracted from each tube and transferred to a 96-well plate and the absorbance value was read at 562 nm. The average triplication readings were then plotted against the concentration of chitosan.

Table.1 Solution usage in ninhydrin assay

Tube ID	1	2	3	4	5
Chitosan solution (mL)	0	0.5	1.0	1.5	2.0
Distilled water (mL)	2	1.5	1.0	0.5	0.0
Ninhydrin solution (mL)	1.0	1.0	1.0	1.0	1.0
Ethanol (mL)	2.0	2.0	2.0	2.0	2.0
Chitosan concentration (mg/mL)	0	0.01	0.02	0.03	0.04

3.4.4 Determination of proanthocyanidins concentration in grape seed extract

3.4.4.1 Preparation of catechin standard curve

Commercial (+)-Catechin hydrate was purchased from Sigm-aldrich (St. Louis,MO). Catechin stock solution was prepared by dissolving 100 mg catechin in 10 mL 75% methanol solution. Then a series of catechin solutions ranging from 0.01 mg/ml to 0.2 mg/ml were prepared though series dilution in micro tubes. Total volume in each micro tube was maintained at 1ml. The head space of tubes was flushed with nitrogen gas and the tube was enclosed with a screw cap and wrapped with aluminum foil to protect from light oxidation. The catechin solution was transferred into cuvettes and the absorbance was measured at 280 nm using a UV-vis spectrophotometer (Perkin Elmer) located at Center for Functional Nanomaterials of Brookhaven National Lab.

3.4.4.2 Measurement of catechin content in grape seed extract

Grape seed extract solutions (40 mg/mL, 100 mg/mL, 200 mg/mL, 300 mg/mL and 400 mg/mL) were prepared as previously mentioned. Then they were diluted through a serial dilution until the absorbance value was within the limits of detection of UV-vis spectrophotometer. The total PAC concentrations were determined using the catechin standard curve and quantitated as mg (catechin equivalence) / mL.

3.4.4.3 Preparation of proanthocyanidin standard curve

10 mg/mL, 5 mg/mL, 2.5 mg/mL, 1 mg/mL, 0.5 mg/mL and 0.2 mg/mL PAC solutions were prepared. And their absorbance values at 562 nm were tested. Absorbance values against their corresponding concentration were plotted.

3.5 Releasing kinetics of PAC from PAC-loaded CSNP

CSNP and PAC-loaded CSNP were prepared as described in Section3.1 and 3.3. Then both of them were suspended in 25 mL DI water in 50 mL BD Falcon™ Conical Tubes. At each time point, the solutions were centrifuged and the supernatants were aspirated. The absorbance values of the supernatants were measures in triplication. The new 25 mL DI water was added and suspended by vortexing. The time points were selected as hour 1, 3, 8, 20, 26, 32, 44, 50 and 56. The absorbance values were plotted against time.

3.6 Bacterial cell cultures

The biofilm-forming bacteria, *Pseudomonas syringae* pv. *papulans* (Psp), were generously donated by Professor Thomas Burr (Cornell University). Two strains, Psp-32 Mutsu apple fruit lesion and Psp-37 Mutsu apple fruit lesion, were tested. The former one is sensitive to streptomycin while the latter one is resistant to streptomycin.

Pseudomonas agar F plates were used to culture Psp bacteria. Basically, 5 mL glycerol (Glycerin 1,2,3-Propanetriol, $C_3H_8O_3$, 99%, molecular biology, Sigma-Aldrich Chemical Co.), and 17.5g Pseudomonas agar (HIMEDIAR M120, for fluorescein, VWR. International) were dissolved in 500 millliters DI water and sterilized in an autoclave at 121 Celsius centigrade. After the solution cooled down to 50 Celsius centigrade, it was poured into 20 sterile polystyrene plates respectively (Fisherbrand Sterile 100 mm × 15 mm polystyrene petri dish). The plates were sealed with parafilm and stored at room temperature. Every four days, one loop of

Pseudomonas syringae pv. *papulans* was transferred to a new agar plate from the old one to maintain the viability of the bacteria..

3.6.1 Growth curve of *Pseudomonas syringae* pv. *papulans*

Growth of *Pseudomonas syringae* pv. *papulans* was measured in the "Terrific Broth" media. Basically, 12 g yeast extract (Bacteriologically tested, ultra-pure grade, Amresco), 6 g tryptone (Microbiologically tested, Sigma-Aldrich), and 2 ml glycerol were dissolved in 450 ml DI water under continuous stirring. The mixture was then sterilized through autoclave (Tuttnauer Autoclave – steam sterilizer, 2540EXA) at 121 °C for 15 minutes and then slowly exhausted. Afterward 6.275 g potassium phosphate dibasic (K_2HPO_4, ≥ 99.9 %, J.T.Baker) and 1.16 g potassium phosphate monobasic (KH_2PO_4, ≥ 99.0%, cell culture tested, Sigma-Aldrich) in 50 ml sterilized water were then added and shaken.

Five full loops of *Pseudomonas syringae* pv. *papulans* were taken from a single agar plate and added to 100 ml fresh Terrific Broth media, followed by vortexing to disperse any clumps. At each time point, an aliquot of 200 µL media was transferred to a 96-well plate in triplication. The optical density of the samples was tested using BIO-TEK plate reader at 562 nm. Pure Terrific Broth media was used as blank control group.

3.7 Anti-biofilm assay

3.7.1 Anti-biofilm property of proanthocyanidin

Three full loops of Psp-32 were added into 20 ml Terrific Broth in a Falcon tube. The bacterial suspension was shaken to be distributed evenly and cultured until it reached an optical

density between 0.1-0.2. Grape seed extract solution (100 mg/ml) was prepared as previous mentioned in section 3.2. Then the solution was filtered with a 0.2 μm syringe filter to yield a 26.36 mg/ml PAC stock solution according to the proanthocyanidins standard curve. Then the bacterial suspension, proanthocyanidins stock and pure Terrific Broth were added in a series of autoclaved glass test tubes (table 2). On Day 5, 200 μL crystal violet solution (0.1% w/v crystal violet in 1 g/L glacial acetic acid) was added to each tube respectively and stained the biofilms for 20 minutes according to O'Toole's protocol [58] with modification. Afterwards, each tube was rinsed with DI water twice to remove any unbound bacteria or crystal violet. The tubes were then air dried and photographs were taken with a digital camera.

Table 2 Solution usages in anti-biofilm property of proanthocyanidns assay

	1	2	3	4	5
Concentration of PAC (mg/ml)	0	1	2.5	5	10
PAC stock needed (μL)	0	78.5	196	393	785
Bacterial suspention (μL)	1000	1000	1000	1000	1000
Pure broth (μL)	5000	4921.5	4804	4603	4215
Total volume (μL)	6000	6000	6000	6000	6000

3.7.2 Anti-biofilm property of bulk chitosan

Psp-32 suspension in Terrific Broth media was prepared as previously mentioned and was used when the optical density reached between 0.1 – 0.2 chitosan solution (2 % w/v prepared in 1 % (v/v) acetic acid) was stirred for 2 hours to dissolve completely. A 100 µL bacterial suspension solution was firstly added to each tube with 1900 µL pure Terrific Broth. Different volumes of 2% chitosan solution were added to each tube and the corresponding volume of 1% acetic acid were also added to maintain the total volume at 2200 µL (table 3).

Table 3 Solution usages in anti-biofilm property of bulk chitosan assay

	1	2	3	4	5
Bacterial suspention (µL)	100	100	100	100	100
Pure broth (µL)	1900	1900	1900	1900	1900
Chitosan solution (µL)	200	100	50	0	0
Acetic acid (µL)	0	100	150	200	0
Distilled water (µL)	0	0	0	0	200
Total volume (µL)	2200	2200	2200	2200	2200

3.7.3 Anti-biofilm property of chitosan-TPP nanoparticles

Three full loops of Psp-32 were added into 20 ml Terrific Broth in a polypropylene tube. The bacterial suspension was used when reached an optical density between 0.1-0.2. A 100 mg/ml chitosan-TPP nanoparticle solution was prepared and sonicated for 10 minutes before being added to the bacterial suspension. Pure broth, bacterial suspension and CSNP stock solutions were mixed as Table 4 shown. On Day 5, the biofilm forming around the tube walls was stained by crystal violet as described previous protocol in section 3.6.1.

Table 4 Solution usages in anti-biofilm property of chitosan-TPP nanoparticle assay

	1	2	3	4	5
Concentration of CSNP (mg/ml)	0	1	2.5	5	10
CSNP stock volume (µL)	0	20	50	100	200
Bacterial suspention (µL)	400	400	400	400	400
Pure broth (µL)	1600	1580	1550	1400	4215
Total volume (µL)	2000	2000	2000	2000	2000

3.7.4 Anti-biofilm property of PAC-loaded chitosan nanoparticles

Bacterial suspension solutions were prepared as previously mentioned in section 3.5.1. Proanthocyanidin-loaded chitosan nanoparticles were resuspended in 9 ml Terrific Broth. The

bacterial suspension (0.2 ml), PAC-loaded chitosan nanoparticle solution (3 mL) and pure Terrific Broth (2.8 mL) were mixed. After five days, the tubes were stained by crystal violet solution and rinsed with DI water.

3.8 Viability assay

The effect of proanthocyanidins, chitosan nanoparticles and PAC-loaded chitosan nanoparticles against the viability of bacteria was evaluated by measuring the zone of inhibition around the drug-loaded bandages.

3.8.1 Zone of inhibition

One loop of Psp from agar F plates was spread out evenly over each new agar F plate. Each unloaded bandage or bandage loaded with chitosan nanoparticles, proanthocyanidins or proanthocyanidin-loaded chitosan nanoparticles was then placed over the center of the plate. The plates were scanned using a photo scanner on a daily basis and the inhibition zones were measured from four directions as Fig.7 shown. Distances a, b, c, and d were measured and averaged.

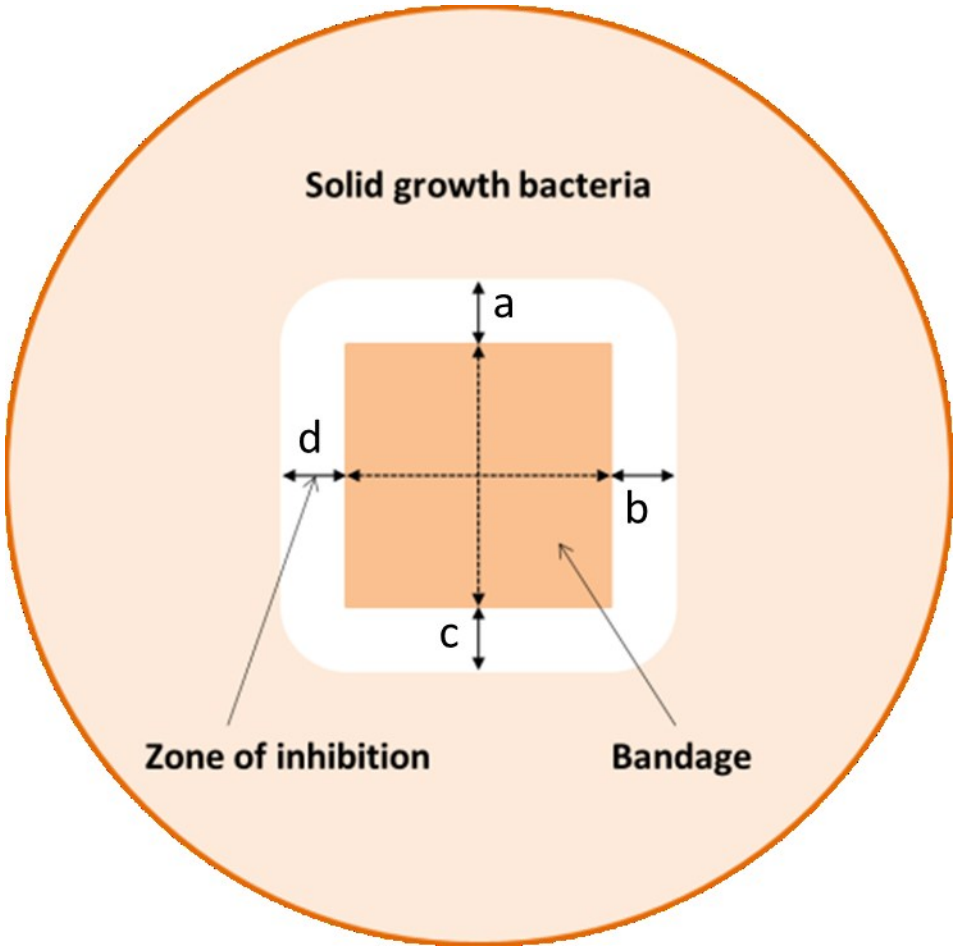

Fig.7 Schematic diagram of the measurement of zone of inhibition

4 Results

4.1 Physical characterization of nanoparticles

4.1.1 Particle size

The average diameter of chitosan-TPP nanoparticles was 236.0 nm (+/-2.4 nm). And after being suspended in DI for 5 days, the average diameter of the chitosan-TPP nanoparticles was increased slightly to 276.3 nm (+/-2.4 nm). The average diameter of PAC-loaded chitosan-TPP nanoparticles was 382.3 nm (+/- 7.0 nm).

Table 5 The size of nanoparticles

Particle	Diameter (nm)
Chitosan-TPP nanoparticles (as-prepared)	236.0±2.4
Chitosan-TPP nanoparticles (after 5 days)	276.3±2.4
PAC-loaded chitosan nanoparticles (as-prepared)	382.3±7.0

		Size (d.nm):	% Intensity:	St Dev (d.nm):
Z-Average (d.nm): 232.6	Peak 1:	288.1	100.0	110.8
PdI: 0.196	Peak 2:	0.000	0.0	0.000
Intercept: 0.951	Peak 3:	0.000	0.0	0.000
Result quality : Good				

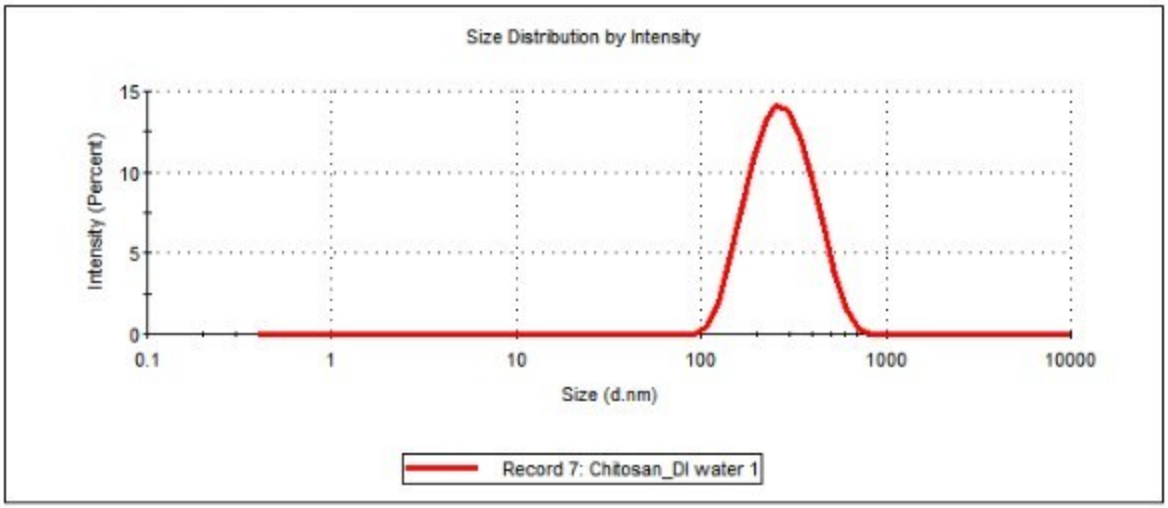

Fig .8 The size distribution by intensity of chitosan nanoparticles

		Size (d.nm):	% Intensity:	St Dev (d.nm):
Z-Average (d.nm): 278.7	Peak 1:	330.4	95.1	146.3
PdI: 0.329	Peak 2:	59.46	2.4	13.36
Intercept: 0.949	Peak 3:	5372	1.6	327.3
Result quality : Good				

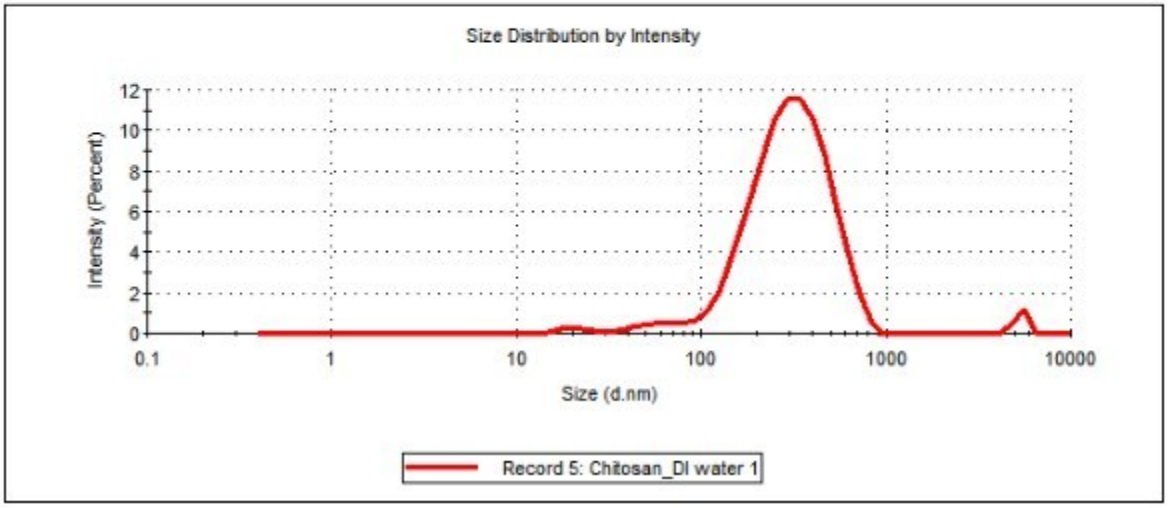

Fig.9 The size distribution by intensity of chitosan nanoparticles

		Size (d.nm):	% Intensity:	St Dev (d.nm):
Z-Average (d.nm): 392.1	Peak 1:	431.9	96.3	236.0
PdI: 0.558	Peak 2:	5446	2.6	271.2
Intercept: 0.964	Peak 3:	21.58	1.1	3.992
Result quality : Good				

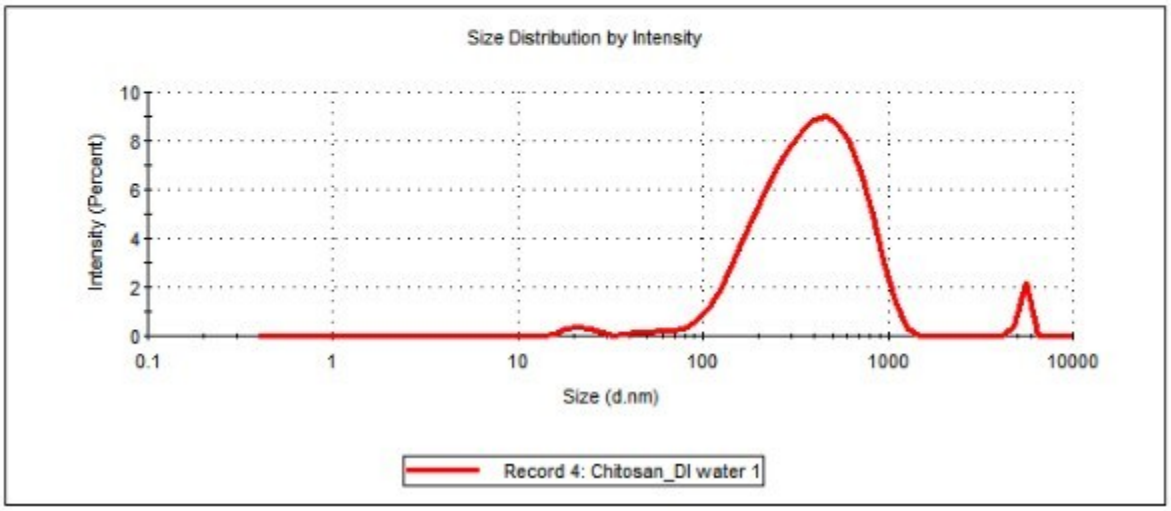

Fig.10 The size distribution by intensity of PAC-loaded chitosan nanoparticles

4.1.2 Zeta potential

Zeta potential is a measurement of the surface charge of the target particle. Particles with a higher zeta potential are electronically stabilized but particles with a lower zeta potential tend to aggregate. Moreover, because cell membrane is negatively changed, thus nanoparticles with a net positive charge are expected to interact better with the target.

As shown in Figure 10, the average zeta potential of 1 mg/mL chitosan-TPP nanoparticles suspended in DI water is plus 29.0 mV (+/- 0 mV), which keeps the nanoparticles moderately stable in water. The average zeta potential of PAC-loaded chitosan-TPP nanoparticles suspended in DI water is plus 31.1 mV (+/- 0.4mV).

Table 6 The zeta potential of nanoparticles

Particle	Zeta potential (mV)
Chitosan-TPP nanoparticles (as-prepared)	29.0 ± 0.0
PAC-loaded chitosan nanoparticles (as-prepared)	31.1 ± 0.4

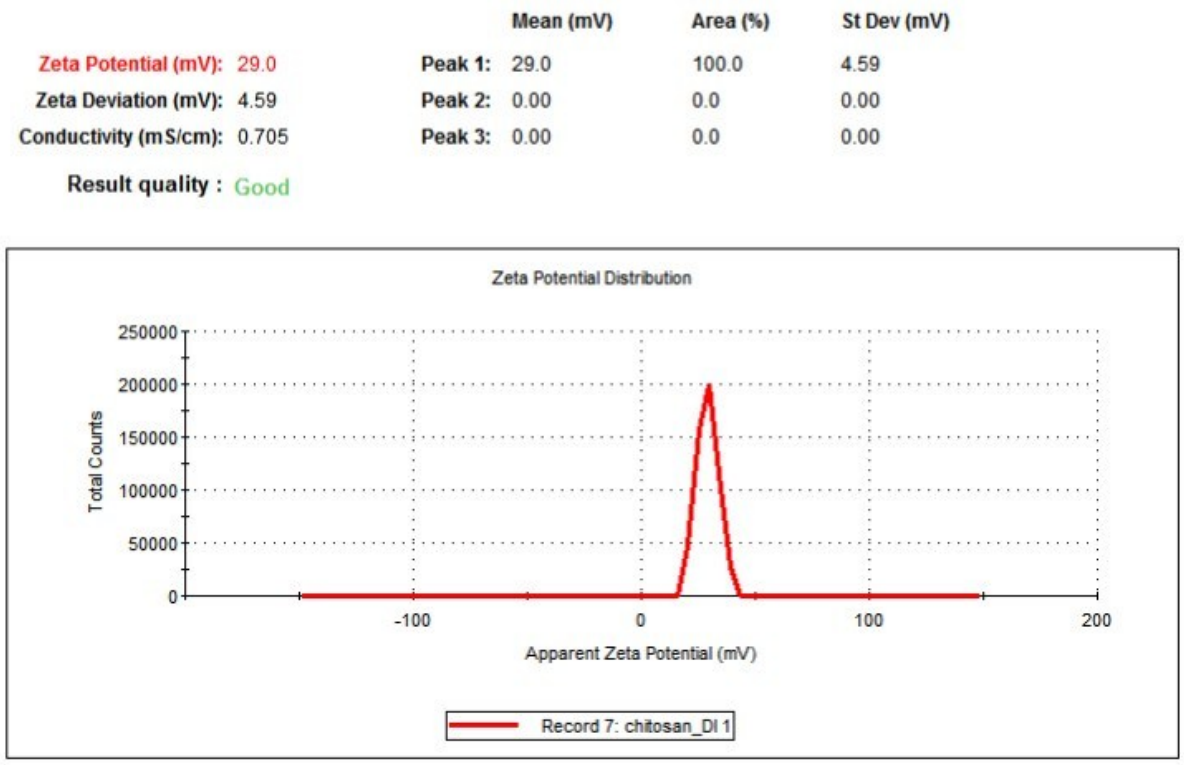

Fig.11 Zeta potential distribution of chitosan nanoparticles

4.1.3 Transmission electron microscope image of PAC-loaded CSNPs

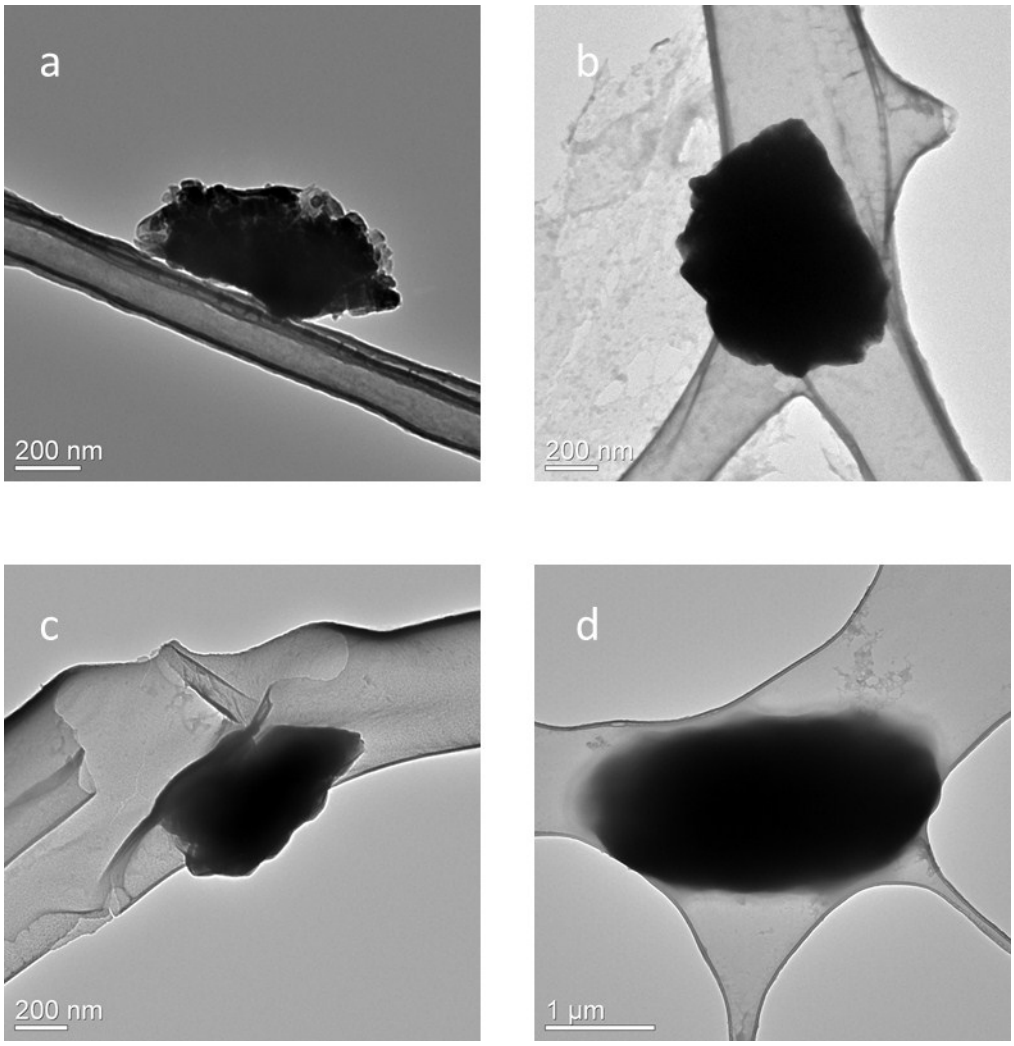

Fig.12 TEM images of PAC-loaded CSNPs.

As Fig.12 shown, most of the PAC loaded chitosan-TPP had the diameter between 350 and 800nm (a,b,c). A minor portion had the diameter between 2µm and 6µm (d). This is in accord with the data from DLS (Fig.10)

4.2 Proanthocyanidins concentration in grape seed extract

4.2.1 Standard curve of catechin

The measured data on the relationship between absorbance at 280 nm and the concentration of catechin is shown in Figure 13 below. A clear absorbance peak can be observed at 280 nm and augmented monotonically with the increase of catechin concentration. The figure showed a linear relation of Y = 13.124*X + 0.036. Thus absorbance value at 280 nm is a reliable method to quantitate the concentration of catechin.

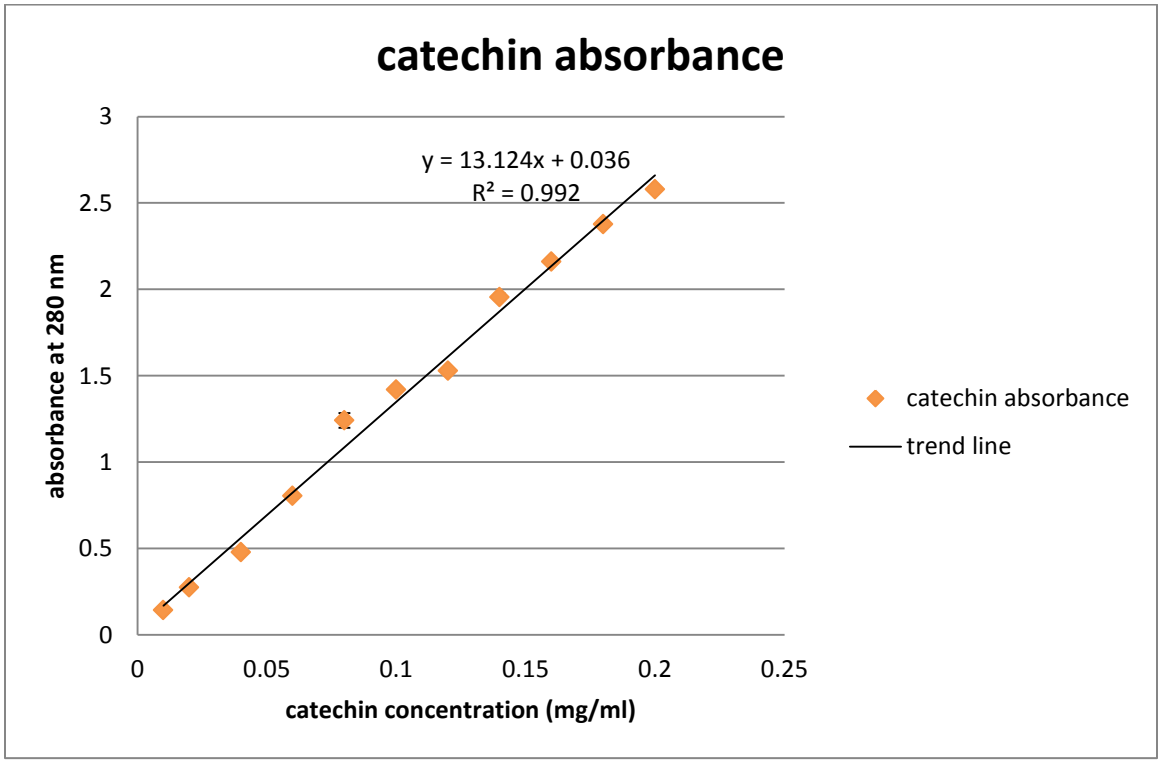

Fig.13 The relationship between absorbance at 280 nm and concentration of catechin (mg/ml)

4.2.2 Standard curve of proanthocyanidins

The measured data on the relationship between absorbance at 562 nm and the concentration of catechin is shown in Figure 14 below. A clear absorbance peak can be observed at 280 nm and augmented monotonically with the increase of catechin concentration. The figure showed a linear relation of Y = 0.0609*X. Thus absorbance value at 562 nm is therefore aan alternative method to quantitate the concentration of PAC.

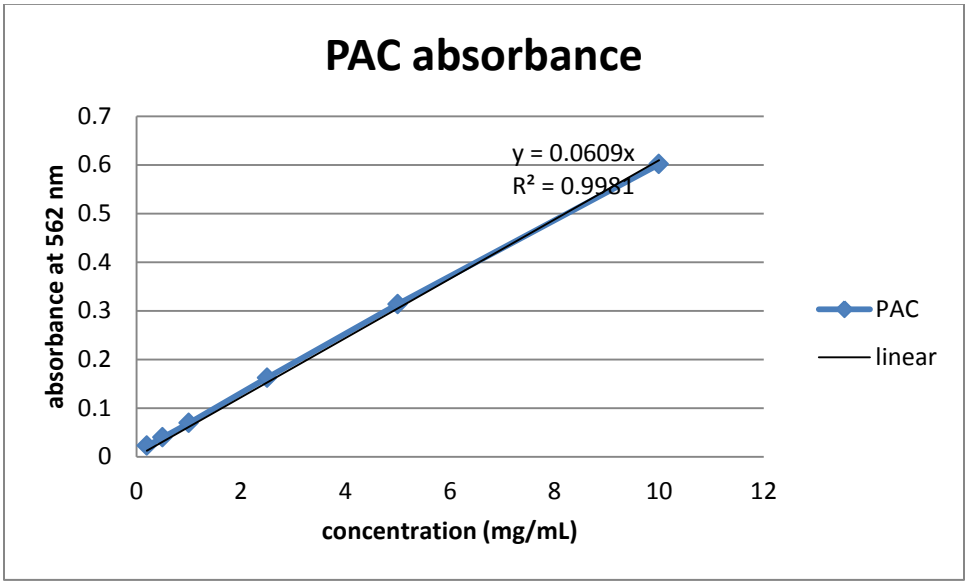

Fig.14 The relationship between absorbance at 562 nm and concentration of PAC (mg/ml)

4.2.3 Proanthocyanidin concentration

The proanthocyanidins solution also showed an obvious absorbance peak at 280 nm, which demonstrated that catechin standard curve is a suitable method for determining proanthocyanidins concentration. The absorbance values of dilutions from 40 mg/mL, 100 mg/mL, 200 mg/mL, 300 mg/mL and 400 mg/mL grape seed extract were measured. Then concentrations of proanthocyanidins were determined through catechin standard curve. The

relationship between concentration of proanthocyanidins (mg/ml) and concentration of grape seed extract (mg/ml) was then plotted as shown Fig.15. In the following anti-biofilm and antibacterial experiment, 100 mg/mL and 400 mg/mL grape seed solutions were used. They were equivalent to 26.2 mg/mL and 76.2 mg/mL PAC, respectively.

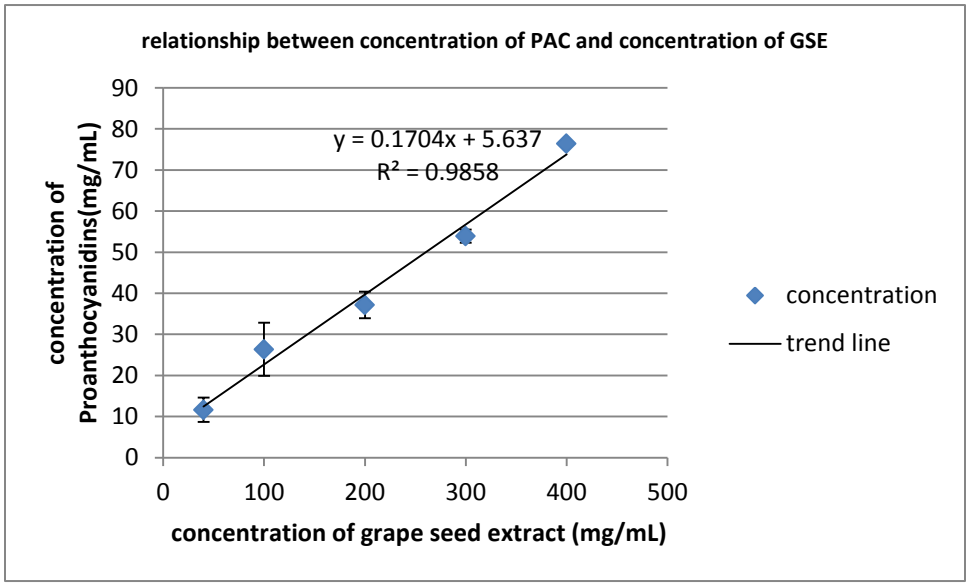

Fig.15 The relationship between concentration of proanthocyanidins (mg/ml) and concentration of grape seed extract (mg/ml)

4.3 Chitosan concentration in chitosan-TPP nanoparticles

The ninhydrin assay yielded a standard curve to determine the concentration of chitosan (Fig.16). It showed a linear relationship between the absorbance and chitosan concentration. Through this assay, 1 mg/mL chitosan-TPP nanoparticle suspension was detected containing 0.11 mg/mL chitosan.

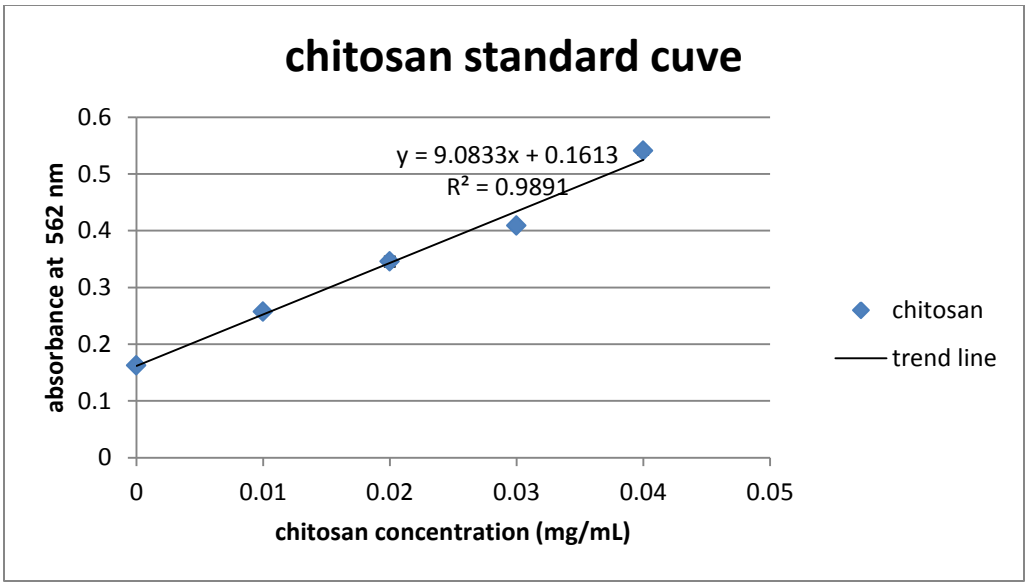

Fig.16 chitosan concentration standard curve

4.4 Release kinetics of PAC from CSNP

From the diagram, we can observe that PAC was stably releasing within 56 hours of incubation in water at room temperature. Using the PAC standard curve (Fig.15), the amount of PAC released into the medium from loaded CSNP was measured to be 1.33 mg/mL within first hour and 5.85 mg/mL within 58 hours. A concentration of above 5.00 mg/mL is an efficient concentration to eliminate biofilm according to the biofilm assay (Fig.19).

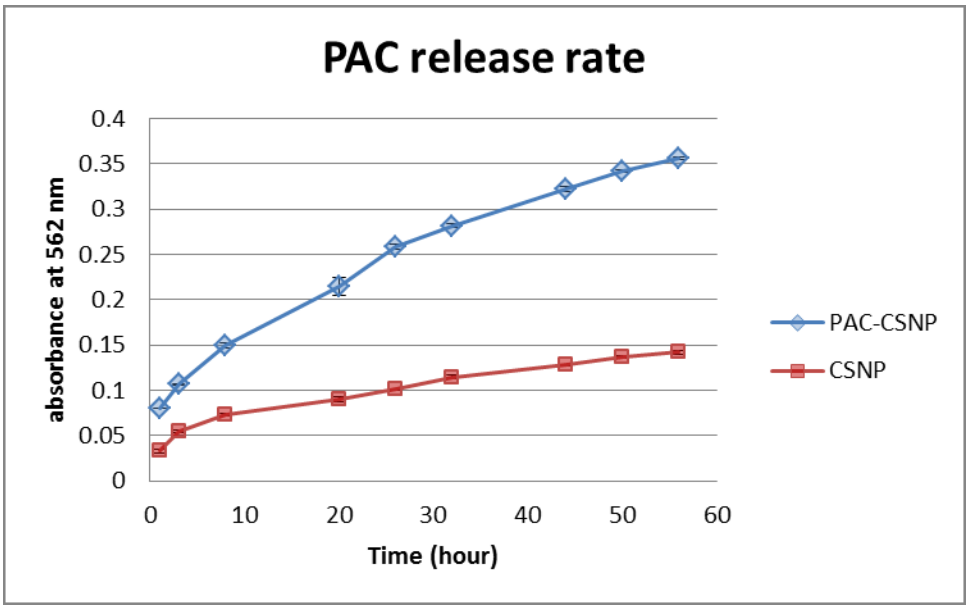

Fig.17 Releasing kinetics of PAC from PAC-loaded CSNP

4.5 Growth curve of *Pseudomonas syringae* pv. *papulans*

The growth curve is shown as Fig.16 below. The time points were selected 0, 4, 8, 16, 20, and 24 hours.

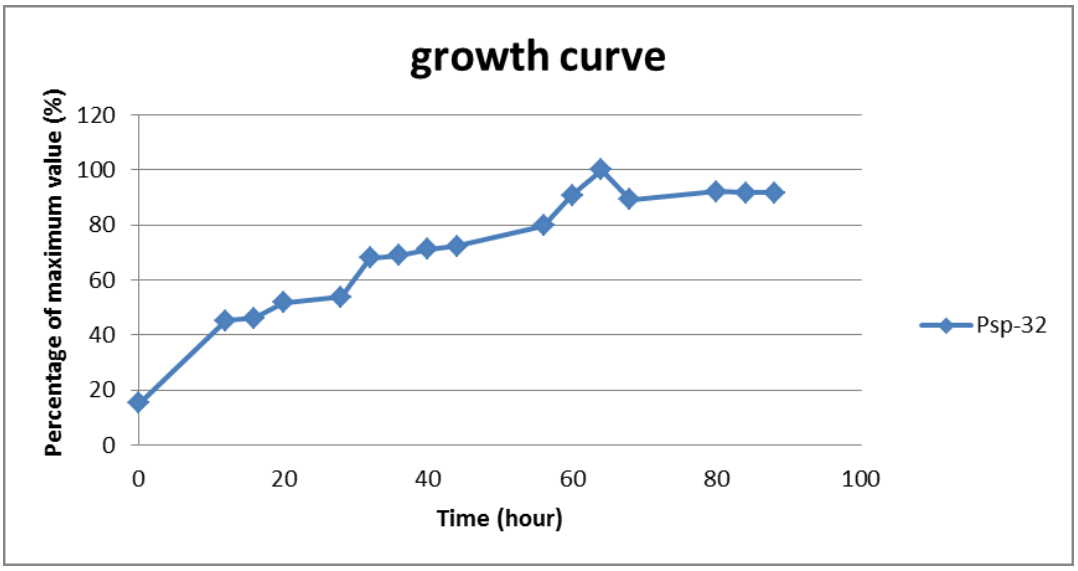

Fig.18 The growth curve of *Pseudomonas syringae* pv. *Papulans* (Psp-32)

The Psp-32 bacteria grew relatively fast in the first 12 hours. This is mainly because when Psp-32 was first exposed to fresh media, after a short period of lag phase, the bacteria began to divide regularly by binary fission. At 64 hours, the bacteria reached its maximum value. After that Psp-32 began to enter its stationary phase and death phase, and the number of viable cells decreased accordingly. But the general four phases (lag phase, exponential or log phase, stationary phase, and death phase) were not very clearly observed. This may be because the optical density test is a turbidimetric method. As the bacteria died, the turbidity did not change, so the death phase may not be accurately assessed.

4.6 Anti-biofilm properties of Proanthocyanidins and Chitosan

4.6.1 Anti-biofilm property of Proanthocyanidins

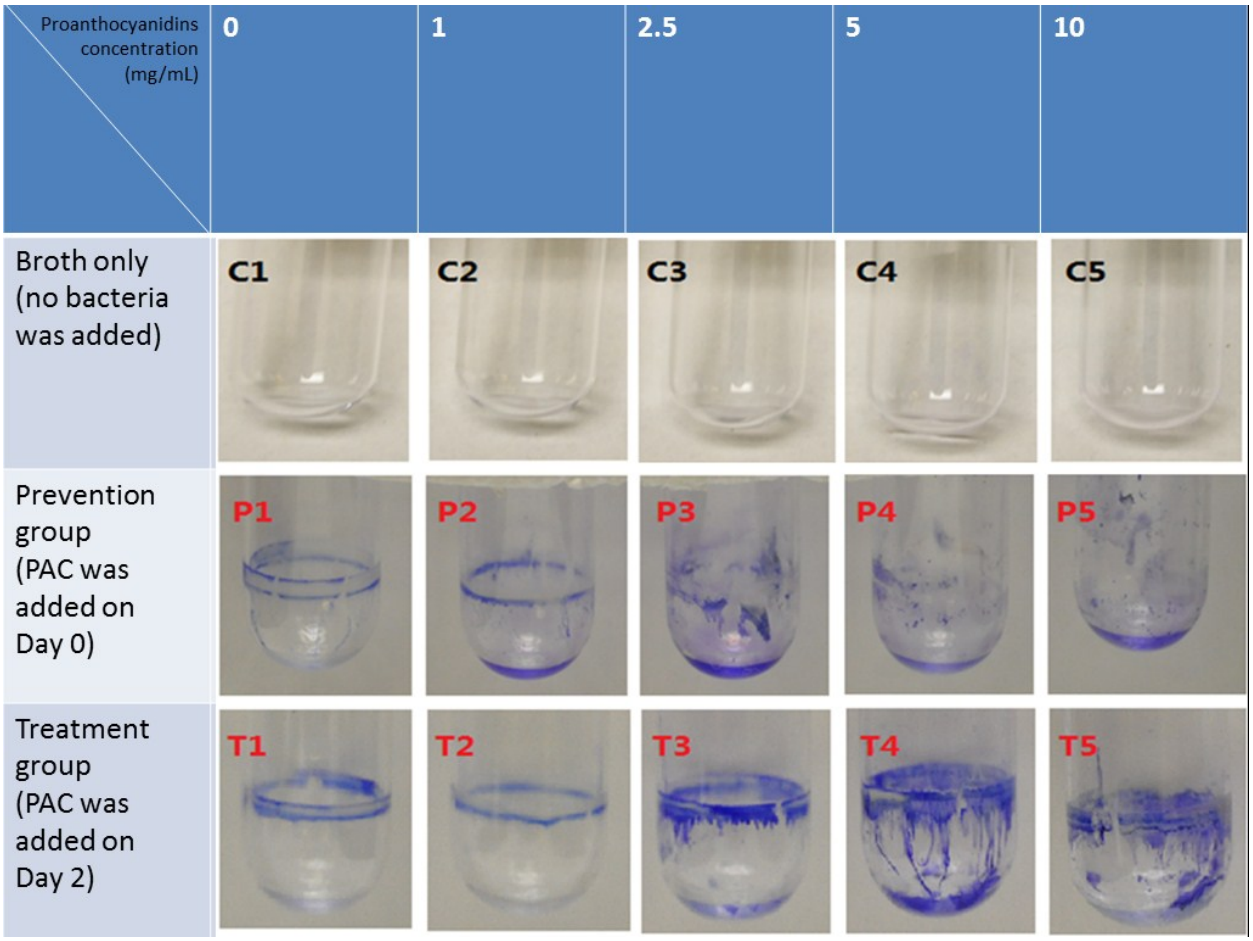

Fig.19 Anti-biofilm property of proanthocyanidins.

As Fig.19 shown, broth only with PAC did not interfere with crystal violet. In the 1 mg/mL proanthocyanidins prevention method, the size of biofilm ring began to decrease. With higher concentration of proanthocyanidins (2.5 mg/mL), biofilm rings around the tube wall were partially distorted (as as P3 shown in Fig.17, panel P3). Compared to prevention method, the treatment method is not satisfactory. Even with the highest PAC treatment method (10 mg/mL), biofilms were only partially distorted.

4.6.2 Anti-biofilm property of bulk chitosan

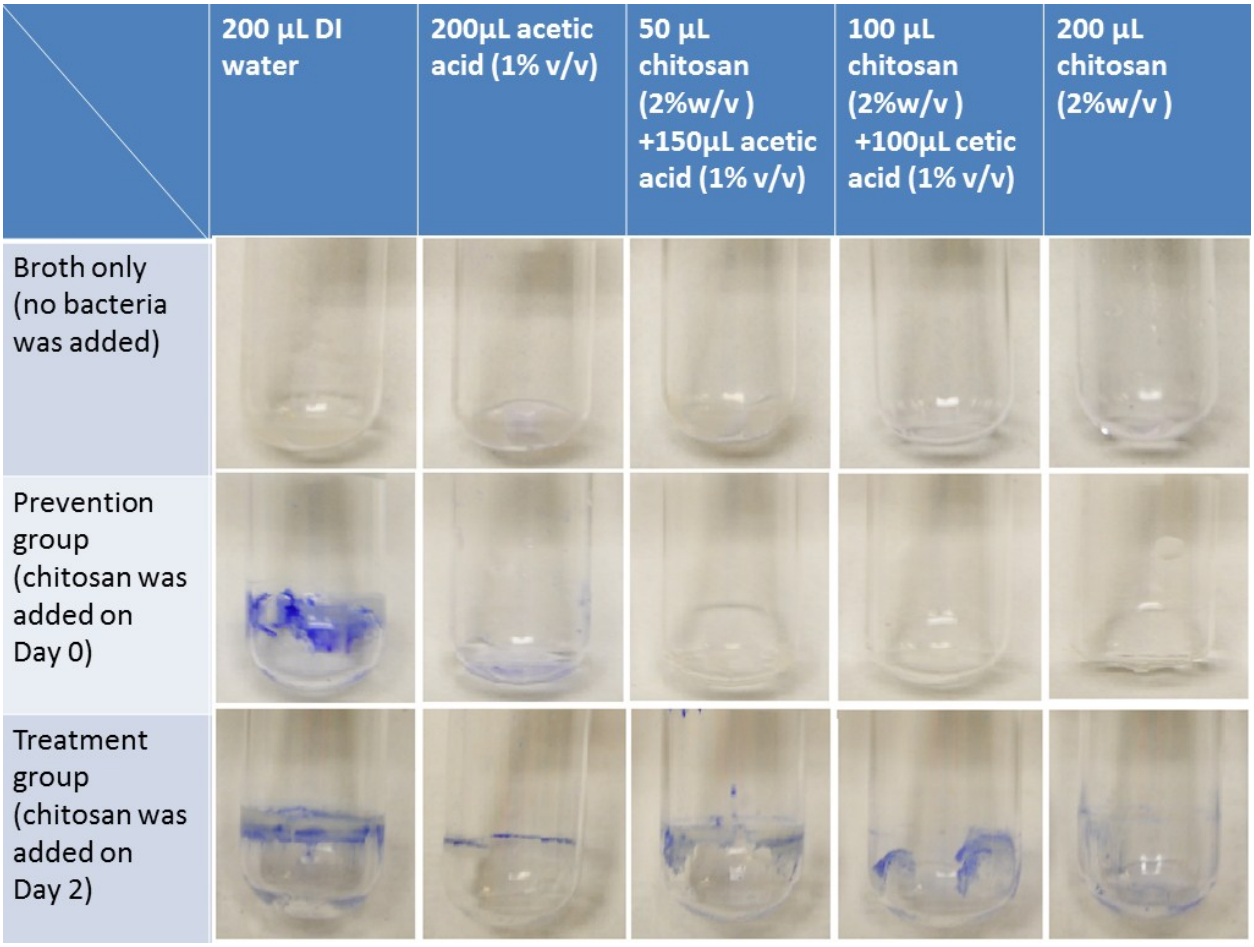

Fig.20 Anti-biofilm property of bulk chitosan.

Broth with bulk chitosan did not interfere with crystal violet (Fig.20). Results showed bulk chitosan may have the ability to disrupt biofilm. However, when only acetic acid was added to the tubes, biofilms were also partially eliminated. The pH value in each tube was also tested before staining. It showed that when bulk chitosan was added, pH value changed from 7~8 to 6~7. Two factors- bulk chitosan and acetic acid affected these tubes. In order to eliminate the factor of pH, water soluble chitosan nanoparticles are needed to eliminate the factor of pH value.

4.6.3 Anti-biofilm property of chitosan-TPP nanoparticles

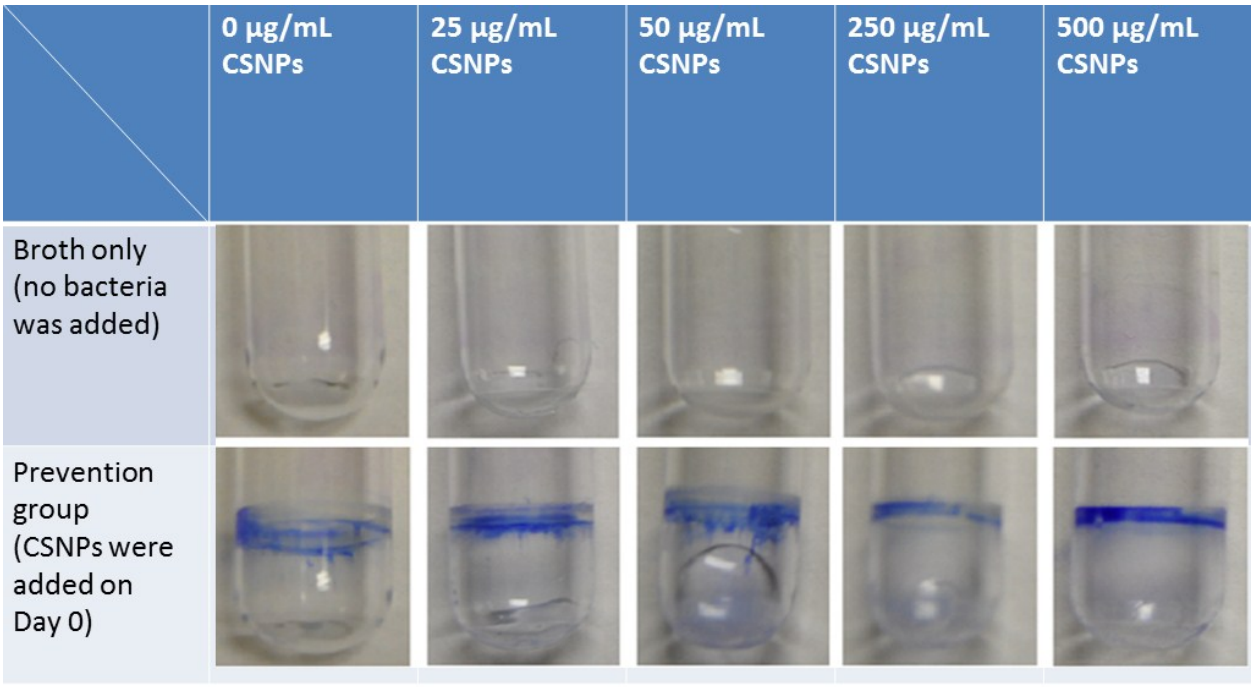

Fig.21 Anti-biofilm property of lyophilized chitosan-TPP nanoparticles P: Prevention method group;PC: Control group

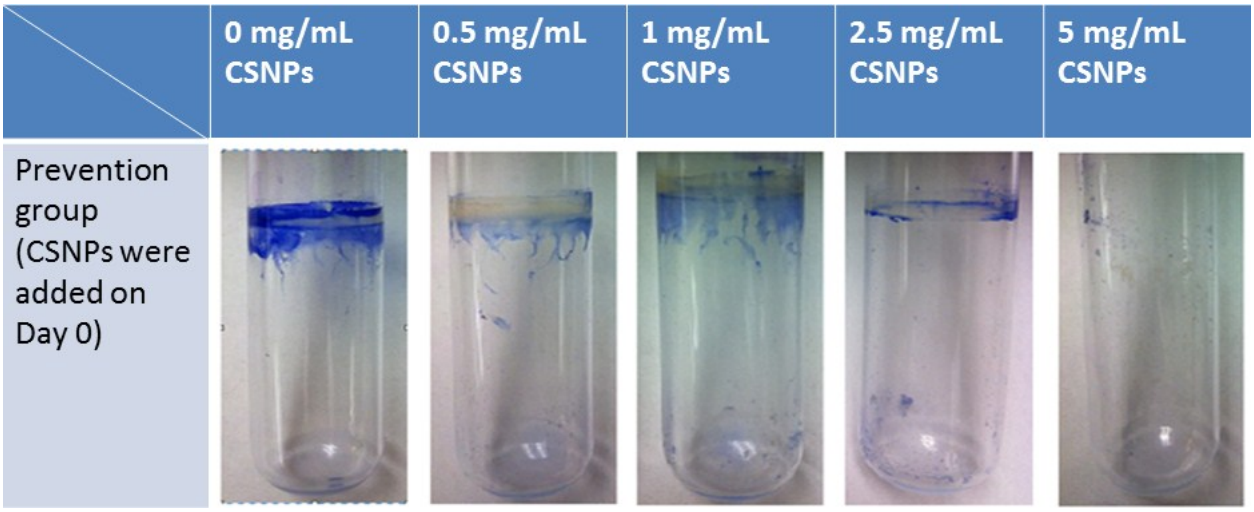

Fig.22 Anti-biofilm property of as-prepared chitosan-TPP nanoparticles. The concentrations of CSNPs are 0, 0.5 mg/ml, 1 mg/ml, 2.5 mg/ml, 5 mg/ml from left to right respectively.

Compared with PAC, The anti-biofilm function of lyophilized CSNPs is not that obvious. The biofilms were only slightly distorted at all concentrations of CSNPs tested. At 25-500 μg/mL of chitosan-TPP nanoparticles, biofilms forming around the tube walls had no difference and were all intact rings after 5 days. When using the as-prepared chitosan nanoparticles, most likely because of a higher chitosan nanoparticles concentration, the biofilms started to be disrupted. As shown in Figure 22, upon 1 mg/ml and 2.5 mg/ml chitosan nanoparticle treatment, sizes of biofilm rings on Day 5 decreased. On 5 mg/ml of chitosan nanoparticle treatment, biofilms were almost eliminated. Broth with chitosan nanoparticle did not interfere with crystal violet (Fig.21)

4.6.4 Anti-biofilm property of PAC-loaded chitosan-TPP nanoparticles

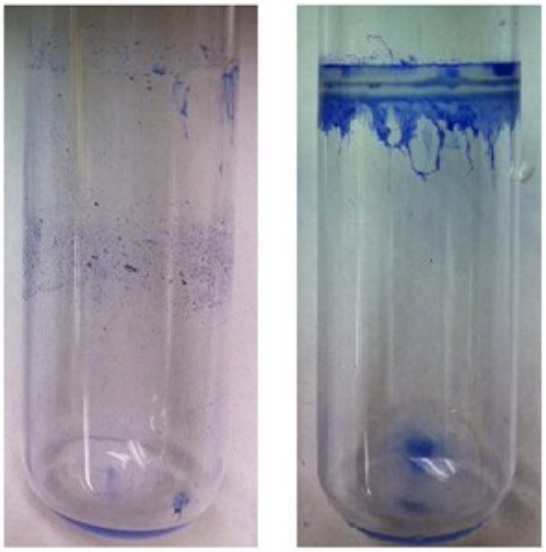

Fig.23 Antibiofilm of PAC-loaded chitosan-TPP nanoparticles. Left: biofilm with PAC-loaded CSNPs treatment. Right: biofilm with no treatment.

Because PAC absorbs in the same optical range as ninhydrin, chitosan concentration cannot be determined by ninhydrin method. So only a group of PAC-loaded CSNPs with unknown concentration is tested for in vitro anti-biofilm assays. With PAC-loaded CSNPs, most biofilms were distorted after five days. (Fig.23)

4.7 Antibacterial properties of proanthocyanidin and chitosan

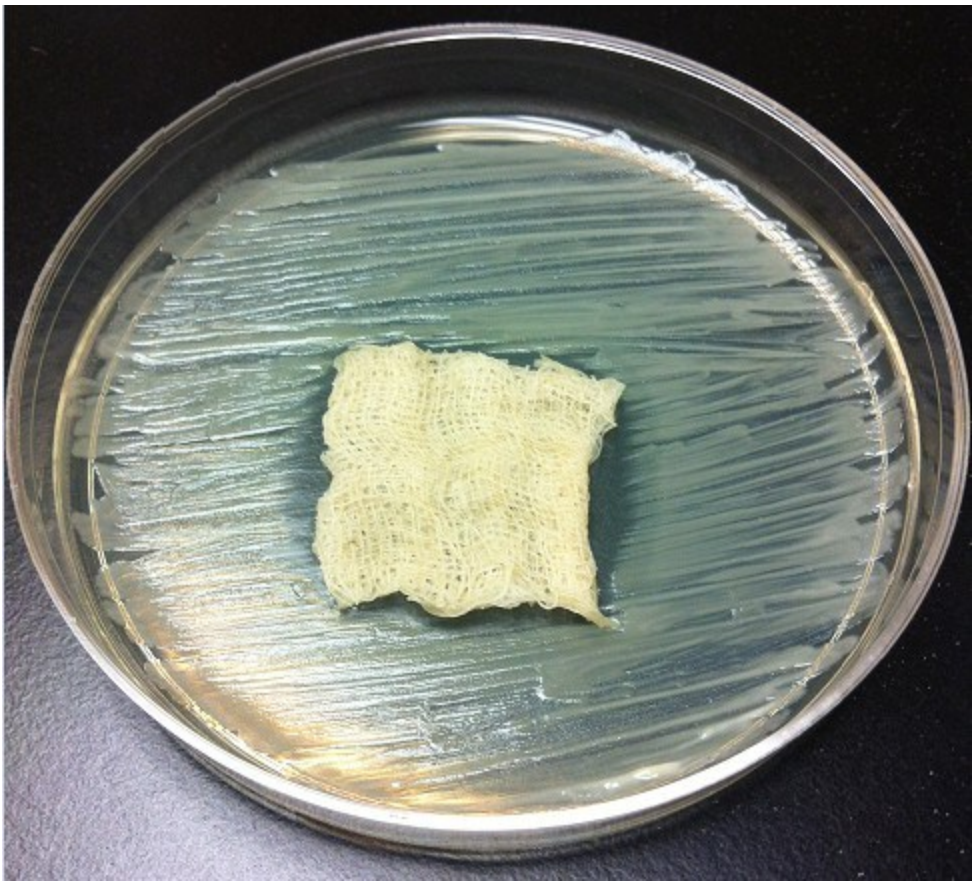

Fig.24 The zone of inhibition around bandage pre-treated with chitosan-TPP nanoparticle on Day 2

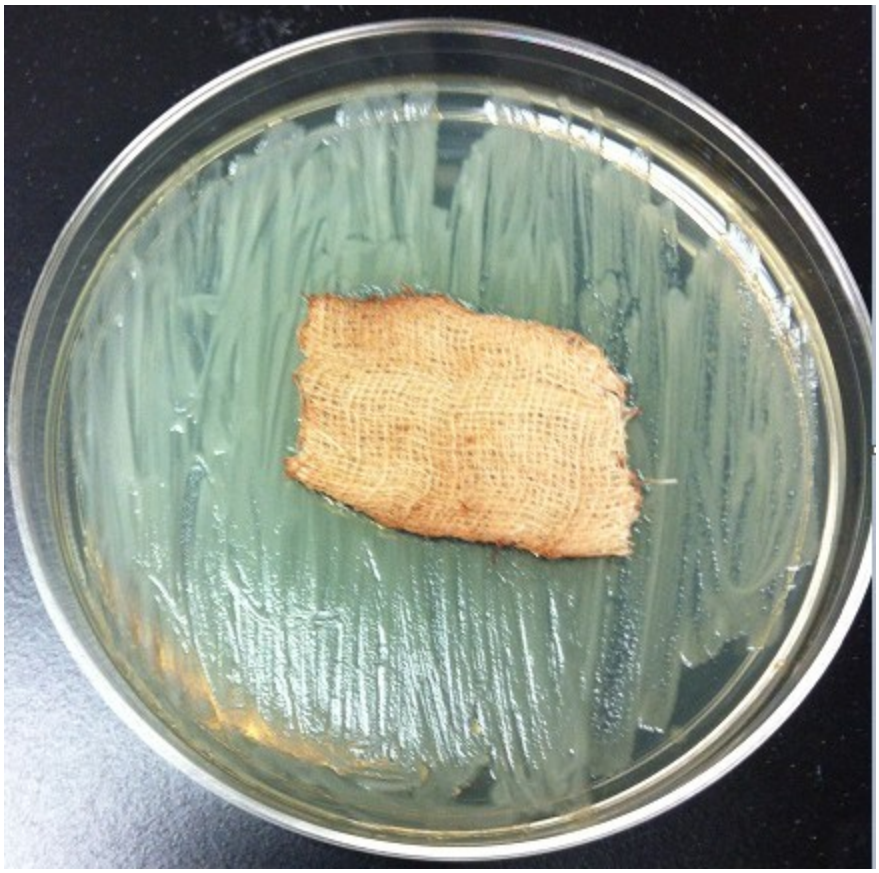

Fig.25 The zone of inhibition around bandage pre-treated with proanthocyanidins on Day 2

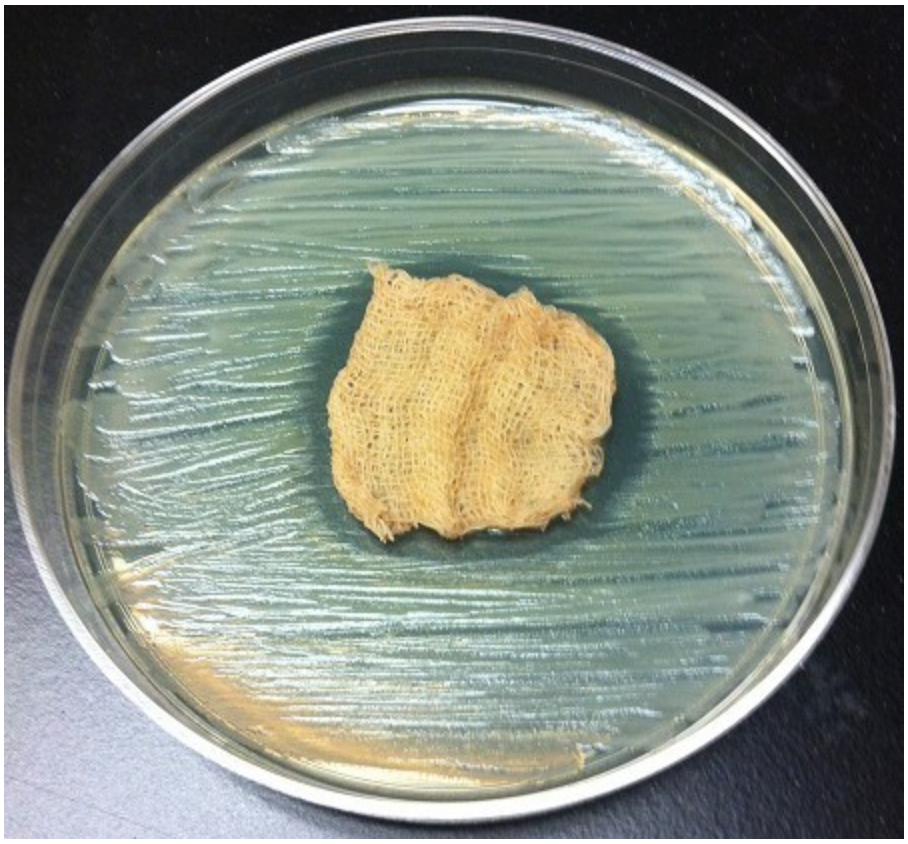

Fig.26 The zone of inhibition around bandage pre-treated with proanthocyanidin-loaded chitosan-TPP nanoparticles on Day 2

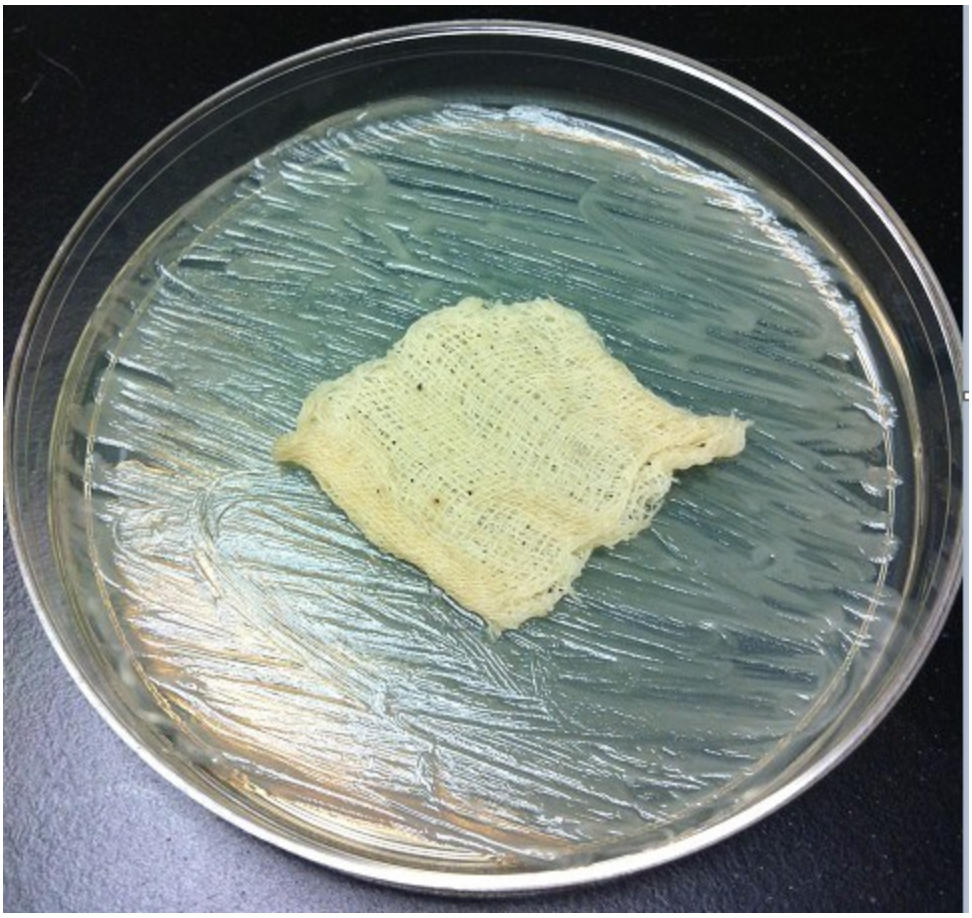

Fig.27 the zone of inhibition was not visible around untreated bandage on Day 2

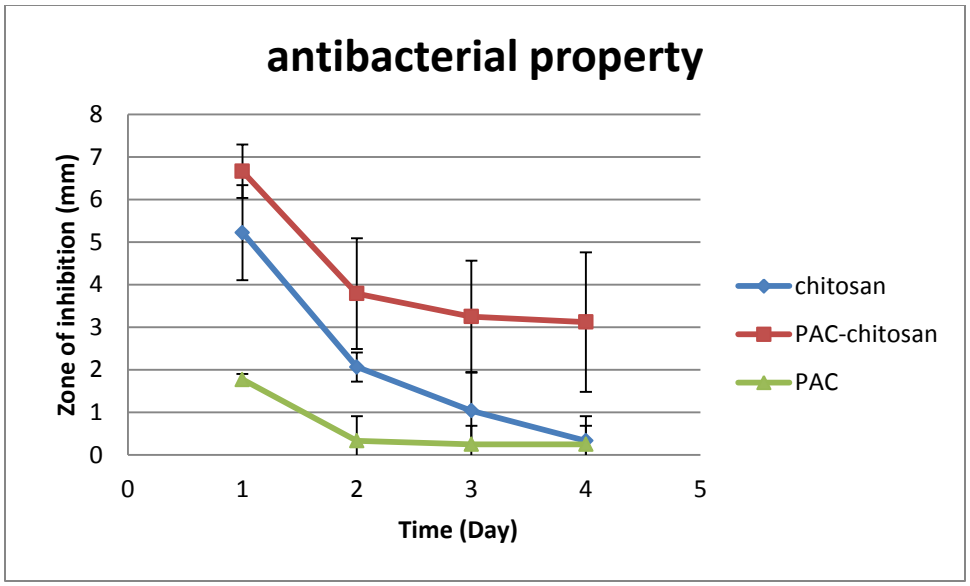

Fig.28 The kinetics of zone of inhibition of drug-loaded bandage

The inhibition zones occurred on Day 1. On Day 1, the average inhibition zone of chitosan nanoparticles is 5.2 mm±1.1 mm; PAC-loaded chitosan nanoparticles 6.7 mm ±0.6 mm; PAC 1.8mm ±0.1 mm (Fig.28) . After Day 1, all the inhibition zones started to decrease till Day 4. Bandages with PAC-loaded chitosan-TPP nanoparticle eventually had an inhibition zone of 3.1 mm ±1.6 mm, whereas bandages with chitosan nanoparticles or proanthocyanidins merely had average inhibition zones of 0.33 mm ±0.57 mm and 0.25mm ± 0.43 mm. After Day 4, the sizes of the zone remained constant. Inhibition zones of control bandage remained zero during the whole test (Fig.28).

5 Discussion

5.1 Anti-biofilm properties of chitosan and proanthocyanidins

The anti-biofilm function of bulk chitosan is limited due to its poor solubility in neutral circumstance. Through ionic gelation method, chitosan formed nanoparticles with sodium tripolyphosphate. The chitosan-TPP nanoparticles have an average diameter of 236.0 nm (+/-2.4 nm) and a plus 29.0 mV (+/- 0.0 mV) surface charge, which give chitosan a better neutral solubility and affinity toward cell membrane of negative charge. Also, the addition of chitosan-TPP suspension to the broth did not change its pH value. Lyophilized chitosan nanoparticles have a good solubility with the addition of trehalose, but it decreased the purity of chitosan.

At lower concentration (1 mg/mL to 2.5 mg/mL), both chitosan nanoparticle and proanthcyanidin can slow down the occurrence of biofilm. Higher concentration of proanthocyanidins (above 5 mg/ml) and chitosan nanoparticles (about 5 mg/ml) would prevent the biofilm thoroughly. This suggests that both biofilm formation is influenced by these two materials in a dose-dependent manner.

It is also observed that proanthocyanidins and as-prepared chitosan nanoparticle worked better against younger biofilms compared to more mature biofilms. That is, when bacteria come in to contact with proanthocyanidins at the start of the growth period, biofilm formation can be postponed or even prevented. But if biofilms are already formed after 1 to 3 days, treatment of proanthocyanidins can only disrupt a small portion of biofilms.

In the growth curve test, a four-phase (lag phase, exponential phase, stationary phase, and death phase) curve was not well observed. Also the biofilm forming around the glass tubes were not firmly attached to the glass tube surface. These result suggested that the pellicle formation

may be involved in the biofilm formation. In that case, pellicle increased the turbidity of the bacterial growth and also lead the instability of the biofilm formation on the tube walls.

5.2 Antibacterial properties of chitosan and proanthocyanidin

In the zone of inhibition test, both chitosan-TPP nanoparticles and PAC-loaded chitosan-TPP nanoparticles showed apparent inhibition zones in the beginning, which proved that both substances have an effective antibacterial property. But after Day 1, the inhibition zone surrounding the chitosan nanoparticle-functionalized bandage began to decrease and within 4 days completely disappeared. The ZoI surrounding functionalized bandage PAC loaded chitosan decreased more slowly and finally stopped around 3.1 mm at Day 4. As prepared chitosan nanoparticles did show an unstable antibacterial property, which proved that chitosan nanoparticles have a better prevention function than inhibition function. This is in accord with chitosan nanoparticles' performance in anti-biofilm assay.

Proanthocyanidin itself also showed mild antibacterial property on Day 1. But its inhibition zone soon disappeared after Day 1 (Fig.28). This is probably because proanthocyanidins can be easily oxidized under the exposure of light and oxygen, even though the samples were covered in aluminum foil. Besides, proanthocyanidins on a bandage have a larger surface area, which would accelerate the oxidation. It is possible that the proanthocyanidins, which is oxidative, can reduce the oxidation-reduction potential (E_h). Jay proposed that aerobic bacteria often require a positive E_h environment for growth, whereas anaerobic bacteria require a negative E_h environment [55]. It may also be the interaction of polyphenol and protein of the membrane disrupt the nutritional transport [56].

When encapsulated in chitosan-TPP nanoparticles, proanthocyanidins exhibited enhanced antibacterial property. The inhibition zone of PAC-loaded chitosan nanoparticles decreased more slowly and remained relative bigger compared with pure PAC or chitosan nanoparticles (Fig.26). This is also confirmed by the PAC release kinetics. From PAC release kinetic curve and PAC standard curve at 562 nm, it is observed that PAC-loaded chitosan nanoparticle can release PAC steadily and finally reach a concentration high enough to eliminate biofilms. Chitosan nanoparticles therefore may act as a vehicle for proanthocyanidin that can slow its overly rapid oxidation and control its releasing rate.

Chitosan and proanthocyanidins both show a limited antibacterial function (chitosan does not have a good solubility and proanthocyanidins can be rapid oxidized). With the coordinating function between proanthocyanidins and chitosan nanoparticle, the antibacterial function is boosted.

Comparing the anti-biofilm assay with the antibacterial assay, some difference could be observed. PAC showed a strong anti-biofilm property but showed a minor antibacterial property. This is probably because PAC was more vulnerable to oxidation when loaded on bandage than dissolved in solution. Chitosan-TPP nanoparticle showed apparent anti-biofilm property above 5 mg/ml. Between 1 mg/ml and 5 mg/ml, CSNP could postpone the formation of biofilm but biofilm could eventually occur on day 5 (Fig.21). That is similar with the antibacterial assay, which chitosan shows a bacterial function at first two days and gradually vanished after Day 2 (Fig.28). There results suggested the anti-biofilm properties of PAC and chitosan-TPP nanoparticle were probably due to their antibacterial functions.

6 Conclusion

In this study, chitosan-TPP nanoparticle and proanthocyanidins-loaded chitosan-TPP nanoparticles were successfully synthesized by the ionic gelation method. Through Dynamic Light Scattering measurement, their diameters were measured to be 236.0 nm (+/-2.4 nm) and 382.3 nm (+/- 7.0 nm), respectively. This is also confirmed through their images of transmission electron microscopy (Fig.12).

Anti-biofilm assay of bulk chitosan showed a good anti-biofilm function. But it is noticed bulk chitosan solution (in 1% acetic acid) changed the pH value of the medium from 7~8 to 6~7. Adding chitosan nanoparticles, proanthocyanidins or proanthocyanidins-loaded chitosan nanoparticle did not change the pH value of the growth medium. At lower concentrations (1 mg/mL and 2.5 mg/mL), both chitosan nanoparticles and proanthocyanidins could postpone the formation of biofilms and eventually disrupted part of the biofilm. At higher concentration (above 5 mg/mL) of chitosan nanoparticles or proanthocyanidins, most of the biofilm was eliminated in this study. PAC-loaded chitosan nanoparticles also could also distort biofilms.

The antibacterial properties of chitosan nanoparticles, proanthocyanidins and proanthocyanidins-loaded chitosan nanoparticle were also tested. Bandages soaked with these three substances were prepared and their zones of inhibition over bacterial agar plates were measured. Proanthocyanidins showed a mild antibacterial property but that property disappeared after 1 day. Chitosan nanoparticle showed a stronger antibacterial property but its property also vanished within 4 days. Bandage pretreated with PAC-loaded chitosan nanoparticles showed a sustaining antibacterial effect even after 4 days. Taken together, these data suggest that chitosan nanoparticles may act as a good anti-oxidation shell carrier for encapsulated proanthocyanidin which may have also prolonged its release and antibacterial effect.

7 Future work

For PAC-loaded chitosan nanoparticles, more methods (HPLC, FTIR etc.) are planned to detect the chitosan concentration in it. The ratio of chitosan and proanthocyanidins can be studied to get an optimal loading efficiency and particle characterization (diameter and zeta potential).

For anti-biofilm assay, more bacterial strains and types of culture media are to be tested to generate more rigid biofilm, which could be further tested by PAC, chitosan-TPP nanoparticles and PAC-loaded chitosan nanoparticles.

For antibacterial assay, the loading efficiency of PAC, CSNP or PAC-loaded CSNP over bandage will be observed, as well as the releasing kinetics of PAC, CSNP or PAC-loaded CSNP.

References

1. Harold C. Neu, "*The crisis in antibiotic resistance*", Science. 257.5073 Aug. , 1992: p1064
2. B.R. Lyon and R. Skurray, Microbiol. Rev 51, 88 (1987).
3. H.C. Neu, in Human Pharmacology, L E. Wingard, Jr., T.M. Brody, J. Lerner, A. Schwartz, Eds. (Mosby-Year Book, New York, 1991), pp. 613-- 698
4. Am. J. Med. 76 (Suppl. 5A), 11 (1984); M. Finland, Rev. Infect. Dis. 1, 14 (1979); D.R. Schaberg et al, Am. J. Med. 70, 445 (1981); D. Milatovic and I. Braveny, Eur. J. Clin. Microbiol. 6, 234 (1987)
5. Sean D. Stowe; Justin J. Richard; Ashley T. Tucker; Richele Thompson, "Anti-Biofilm Compound Derived from Marine Sponge", *Marine Drugs*, **2011**, 9, 2010-2035; doi: 10.3390/md9102010
6. Qian, P.Y.; Lau, S.; Dahms, H.U.; Dobretsov, S.; Harder, T. Marine biofilms as mediators of colonization by marine macroorganisms: Implications for antifouling and aquaculture. *Mar. Biotechnol.* **2007**, 9, 399–410.
7. Beech, I.B.; Sunner, J. Biocorrosion: Towards understanding interactions between biofilms and metals. *Curr. Opin. Biotechnol*. **2004**, 15, 181–186.
8. Costerton, J.W.; Lewandowski, Z.; Caldwell, D.E.; Korber, D.R.; Lappin-Scott, H.M. Microbial biofilms. *Annu. Rev. Microbiol*. **1995**, 49, 711–745.
9. Costerton, J.W.; Stewart, P.S.; Greenberg, E.P. Bacterial biofilms: A common cause of persistent infections. *Science* **1999**, 284, 1318–1322.
10. Sauer, K.; Camper, A.K.; Ehrlich, G.D.; Costerton, J.W.; Davies, D.G. "Pseudomonas aeruginosa displays multiple phenotypes during development as a biofilm". J. *Bacteriol*. **2002**, 184, 1140–1154.
11. Davey, M.E.; O'Toole, G.A. "Microbial biofilms: from ecology to molecular genetics". *Microbiol. Mol. Biol*. Rev. **2000**, 64, 847–867.
12. Blazquez, J. "Hypermutation as a factor contributing to the acquisition of antimicrobial resistance". *Clin. Infect. Dis.* **2003**, 37, 1201–1209.
13. Hausner, M.; Wuertz, S. "High rates of conjugation in bacterial biofilms as determined by quantitative in situ analysis". *Appl. Environ. Microbiol.* **1999**, 65, 3710–3713.
14. Velkov, V.V. "New insights into the molecular mechanisms of evolution: Stress increases

genetic diversity". *Mol. Biol. (Mosk.)* **2002**, 36, 209–215.

15. Costerton, J.W.; Cheng, K.J.; Geesey, G.G.; Ladd, T.I.; Nickel, J.C.; "Dasgupta, M.; Marrie, T.J. Bacterial biofilms in nature and disease". *Annu. Rev. Microbiol.* **1987**, 41, 435–464.
16. Purevdorj-Gage, B.; Costerton, W.J.; "Stoodley, P. Phenotypic differentiation and seeding dispersal in non-mucoid and mucoid Pseudomonas aeruginosa biofilms". Microbiology, 2005, 151, 1569–1576.
17. Keren, I.; Kaldalu, N.; Spoering, A.; Wang, Y.; Lewis, K. "Persister cells and tolerance to antimicrobials". *FEMS Microbiol. Lett.* **2004**, 230, 13–18.
18. Lewis, K. Riddle of biofilm resistance. Antimicrob. *Agents Chemother.* **2001**, 45, 999–1007.
19. Spoering, A.L.; Lewis, K. Biofilms and planktonic cells of pseudomonas aeruginosa have similar resistance to killing by antimicrobials. *J. Bacteriol*. **2001**, 183, 6746–6751
20. Joachim Klahre; H-C Flemming, "Monitoring of biofouling in papermill process waters", *Water Research,* **2000**, Vol. 34, No. 14, pp. 3657±3665, 2000
21. Characklis, W.G.; James, D.; Bryers, I.B. "Bioengineering report: Fouling biofilm development: A process analysis". *Biotechnol. Bioeng*. **2009**, 102, 309–347.
22. Chambers, L.D.; Stokes, K.R.; Walsh, F.C.; Wood, R.J.K. "Modern approaches to marine antifouling coatings". *Surf. Coat. Technol.* **2006**, 201, 3642–3652.
23. Kumar, C.G.; Anand, S.K. "Significance of microbial biofilms in food industry: A review". *Int. J. Food Microbiol*. **1998**, 42, 9–27.
24. "Research on microbial biofilms (PA-03-047)". NIH, National Heart, Lung, and Blood Institute. 2002-12-20.
25. Rogers A H. "Molecular Oral Microbiology". *Caister Academic Press*. pp. 65–108. **2008**, ISBN 978-1-904455-24-0
26. Costerton, J. W.; Stewart, P. S. & Greenberg, E. P. Bacterial biofilms: a common cause of persistant infections. Science 284, 1318– 1322 (1999).
27. Burns, J. L. , Ramsey, B. W. & Smith, A. L. Clinical manifestations and treatment of pulmonary infections in cystic fibrosis. Adv. Pediatr. Infect. Dis. 8, 53–66 (1993).
28. Hoiby, N. Antibiotic therapy for chronic infection of Pseudomonas in the lung. Annu. Rev. Med. 44, 1– 10 (1993).
29. Costerton, J. W. , Lewandowski, Z. , Caldwell, D. E. , Korber, D. R. & Lappin-Scott, H. M. Microbial biofilms. Annu. Rev. Microbiol. 49, 711–745 (1995).

30. Bandyk, D.F.; Esses, G.E. Prosthetic graft infection. *Surg. Clin. North Am.* **1994**, 74, 571–590
31. Francisco Antonio Guardiola, Alberto Cuesta, José Meseguer and Maria Angeles Esteban, "Risks of Using Antifouling Biocides in Aquaculture", *Int. J. Mol. Sci.* **2012**, 13, 1541-1560; doi:10.3390/ijms13021541
32. Annie Shrestha, Anil Kishen, "Polycationic Chitosan-Conjugated photosensitizer for antibacterial photodynamic Therapy", Photochemistry and Photobiology, 2012, 88: 577-583.
33. Lars Plate, Michael A. Marletta, "Nitric Oxide Modulates Bacterial Biofilm Formation through a Multicomponent Cyclic-di-GMP Signaling Network", *Molecular Cells*, **2012**, Volume 46, Issue 4, Pages 449–460
34. Leonarduzzi, G. "*Design and Development of Nanovehicle-Based Delivery Systems for Preventive or Therapeutic Supplementation with Flavonoids*."CURRENT MEDICINAL CHEMISTRY. 17.1 (2010): 74-95.
35. Mayer, Robert, and Guenther Stecher. "Proanthocyanidins:Target compounds as antibacterial agents." *Journal of agriculture and food chemstry*. 56. (2008): 6959-6966.
36. Souquet, J; Cheynier, Véronique; Brossaud, Franck; Moutounet, Michel (1996). "Polymeric proanthocyanidins from grape skins", Phytochemistry 43 (2): 509. doi: 10.1016/0031-9422(96)00301-9.
37. USDA Database for the Proanthocyanidin Content of Selected Foods – 2004 <http://www.nal.usda.gov/fnic/foodcomp/Data/PA/PA.html>[verification needed][page needed]
38. Sáenz-navajas, M. (2012), "Insights on the chemical basis of the astringency of Spanish red wines", *Food Chemistry*, vol. 134, no. pp. 1484-1493.
39. Shanmuganayagam, D., "Differential Effects of Grape (Vitis vinifera) Skin Polyphenolics on Human Platelet Aggregation and Low-Density Lipoprotein oxidation", *Jounal of Agricultural and Food Chemistry*, 2012, 60, 5787−5794
40. Sivaprakasapillai, B., "Effect of grape seed extract on blood pressure in subjects with the metabolic syndrome", *Metabolism Clinical and Experimental,* 58 (2009) 1743–1746
41. Bravo, L.B. Polyphenols: chemistry, dietary sources, metabolism, and nutritional significance. *Nutr. Rev.*, 1988, 56, 317-33
42. Jayaprakasha, G.; Selvi, T.;Sakariah, K. K. Antibacterial and antioxidant activities of grape

(Vitis vinifera) seed extracts. *Food Res.* Int. 2003, 36, 117-222

43. Plama, M.; Taylor, L. T. Fractional extraction of compounds from grape seeds by supercritical fluid extraction and analysis for antibacterial and agrochemical activities. J. Agric. *Food Chem.* 1999, 47, 5044-5048.
44. Rauha, J.; Remes, S.; Heinonen, M.;Hopia, A. Antibacterial effects of Finish plant extracts containing flavonoids and other phenolic compounds. Int. J. *Food Microbiol*. 2000, 56, 3-12.
45. Robert Mayer, Guenther stecher, "Proanthocyanidins: Target Compounds as Antibacterial Agents", *Agriculture and Food chemistry*, **2008**, 56, 6959-6966
46. Maria Daglia, Monica Stauder, "Isolations of red wine components with anti-adhesion and anti-biofilm activity agaist *Streptococcus mutan*s ", Food Chemistry, 119(2010), 1182-1188
47. Shrestha, Annie; Kishen, Anil, "Polycationic Chitosan-Conjugated Photosensitizer for Antibacterial Photodynamic Therapy", PHOTOCHEMISTRY AND PHOTOBIOLOGY, Volume: 88, Issue: 3, Pages: 577-583,DOI: 10.1111/j.1751-1097.2011.01026.x
48. Chung, YC; Su, YP; Chen, CC; et al., "Relationship between antibacterial activity of chitosan and surface characteristics of cell wall", ACTA PHARMACOLOGICA SINICA, 2004, Volume: 25, Issue: 7, Pages: 932-936.
49. Young, D. H.; Kohle, H.; Kauss, H. Plant Physiol ,1982, 70, 1499–1454
50. Hadwinger, L. A.; Kendra, D. F.; Fristensky, B. W.;Wagoner, W. In Chitin in Nature and Technology;Muzzarelli, R. A. A.; Jeuniaux, C.; Gooday, C., Eds.;Plenum: New York, 1985; p 210.
51. Xiao Fei Liu, Yun Lin Guan, Dong Zhi Yang, Zhi Li, Kang De Yao, "Antibacterial action of chitosan and carboxymethylated chitosan", Journal of Applied Polymer Science, 2001, Volume 79, Issue 7, pages 1324–1335, 14 February 2001.
52. Anil Kishen, Zhilong Shi, Annie Shrestha, Koon Gee Neah, "An investigation on the Antibacterial and Antibiofilm Efficacy and of Cationic Nanoparticles for Root Canal Disinfection", Basic Research-Technology, 2008, Volume 34, Number 12.
53. Jena, Prajna, Mohanty, Soumitra, Mallick, Rojee, "Toxicity and antibacterial assessment of chitosan-coated silver nanoparticles on human pathogens and macrophage cells", INTERNATIONAL JOURNAL OF NANOMEDICINE, 2012, Volume: 7, Pages: 1805-1818.
54. Decker, EM; Weiger, R; Wiech, I; et al., "Comparison of antiadhesive and antibacterial effects of antiseptics on Streptococcus sanguinis", EUROPEAN JOURNAL OF ORAL

SCIENCES, 2003, Volume: 111, Issue: 2, Pages: 144-148.

55. Jay, J. M. (1996). *Modern food microbiology* (5th ed.). New York NY: Chapman and Hall.
56. Cerrutti, P., & Alzamora, S. M. (1996). “Inhibitory effects of vanillin on some food spoilage yeasts in laboratory media and fruit purees”. INTERNATIONAL JOURNAL OF FOOD MICROLOGY, 29, 379 – 386.
57. E. Curotto, F. Aros. “Quantitative Determination of Chitosan and the Percentage of Free Amino Groups”. ANALYTICAL BIOCHEMISTRY, VOLUME 211, ISSUE 2, JUNE 1993, PAGES 240–241.
58. Daniel Kadouri and George A. O'Toole, “Susceptibility of Biofilms to Bdellovibrio bacteriovorus Attack”, ENVIRONMENTAL MICROBIOLOGY, JULY 2005 VOL. 71 NO. 7 4044-4051.
59. QI, L., et al., “Preparation and antibacterial activity of chitosan nanoparticles”. CARBOHYDRATE RESEARCH, 2004. 339: p. 2693-2700.